MINERALOGICAL, GEOCHEMICAL, AND ISOTOPIC EVIDENCE OF DIAGENETIC ALTERATION, ATTRIBUTABLE TO HYDROCARBON MIGRATION, CEMENT-CHICKASHA FIELD, OKLAHOMA

By

RALPH ANTHONY LILBURN

Bachelor of Science

Oklahoma State University

Stillwater, Oklahoma

1979

Submitted to the Faculty of the Graduate College
of the Oklahoma State University
in partial fulfillment of the requirements
for the Degree of
MASTER OF SCIENCE
May, 1981

MINERALOGICAL, GEOCHEMICAL, AND ISOTOPIC EVIDENCE OF DIAGENETIC ALTERATION, ATTRIBUTABLE TO HYDROCARBON MIGRATION, CEMENT-CHICKASHA FIELD, OKLAHOMA

Thesis Approved:

Zuhair al-Shaieb
Thesis Adviser

Nathan L. Green

John W. Shelton

Norman N. Durham
Dean of the Graduate College

PREFACE

The Permian beds of the Cement-Chickasha Oil Field of southwestern Oklahoma have been highly altered. This diagenetic mineralization is an expression of hydrocarbon leakage and accumulation at depth. This relationship between the alteration and petroleum was supported by petrographic studies, scanning electron microscopy, sulphur, carbon, and oxygen isotopic analysis, X-ray diffraction, and detailed examination and description of oil well cuttings.

The author wishes to express his appreciation to his thesis adviser, Dr. Zuhair Al-Shaieb, for his insight and guidance during this study. Appreciation is also expressed to Dr. John W. Shelton and Dr. Nathan Green for serving as advisory committee members. The author wishes to thank Shell Development Company for funding during the study.

A note of thanks is given to the Oklahoma Geological Survey Core Library, and the Shawnee Sample Service for well samples studied during the investigation and to the Oklahoma City Log Library for the use of their electric logs. Thanks is also extended to Ms. Jeanne Vale for typing the final draft.

Special appreciation and thanks is expressed to my parents, Ralph and Pat Lilburn, for their understanding and support, to my sister, Mona Lilburn, for typing earlier drafts of the manuscript, and to my wife, Marxanna, for her encouragement, sacrifices and help too numerous to list.

TABLE OF CONTENTS

LIST OF TABLES

LIST OF FIGURES

Figure Page

LIST OF PLATES

CHAPTER I

INTRODUCTION

The oil field at Cement, Oklahoma, has been the topic of several studies since its discovery in 1916. Initial work involved the fundamental stratigraphy and structure of the field, so further exploration could be attempted more successfully. In his study of the Cement field, Reeves (1922) reported an alteration of the surface Permian beds, which are normally reddish-brown and friable in southwestern Oklahoma. This alteration resulted in a color change of the Rush Springs Sandstone to pink, white, and yellow with an accompanying carbonate cement two-thirds of the way up the topographically expressed structure. Similar alterations were described at other structurally controlled oil fields in southern Oklahoma (Harlton, 1960).

A comprehensive study of the surface alteration on the Cement Anticline was conducted by Donovan (1972). He explained these diagenetic features as evidence of the buried hydrocarbons at depth. Donovan suggested that these color changes were due to the reduction of iron by the migrating hydrocarbons. Carbonate cement collected from the surface sandstone outcrops at Cement was used for carbon and oxygen stable isotope studies. He noticed a strong petroleum influence on the isotopic ratio. These isotopes were affected most over major Pennsylvanian faults and less away from the structures.

Olmstead (1975) related the occurrence of uranium mineralization at

Cement to hydrocarbon migration. This deposit was mined from the crest of the Cement Anticline in the mid-1950's. He also found anomalous concentrations of uranium in ground water associated with several other oil-producing anticlines that had altered beds at their crests.

The geochemical processes outlined by Donovan (1972) for the Cement alteration has been used as a framework model to describe the subsurface alteration of Permian beds in other areas. Ferguson (1977), in his study on four oil fields with structural traps in southwestern Oklahoma, showed that the alteration did extend into the subsurface. He stated that pyrite minereralization occurred over areas of hydrocarbon accumulations. Ferguson (1977) also indicated that this pyrite formed when hydrogen sulfide associated with petroleum reacted with the abundant iron oxide in these red beds.

Allen (1980) further studied the uranium potential of the Cement-Chickasha area. In this study he did extensive surface mapping of the alteration zones.

From the compiled data of all the previous studies completed on the Cement, Oklahoma, oil field and the general area, there is enough evidence to support the claim that this field represents a model of red bed diagenetic alteration caused by structurally controlled hydrocarbon migration. This migration caused three primary results: (1) the sandstones were altered in color, caused by a reducing environment in the presence of H_2S gas (Donovan, 1972), (2) the oxidation of hydrocarbons caused sandstones to be cemented with carbonate, and gypsum to be replaced by calcite over the crest of the anticlines (Donovan, 1972), and (3) pyrite formed in the altered sandstones as a result of a reduction of iron oxide by petroleum related H_2S gas (Ferguson, 1977).

The purpose of this study is to integrate all published data and newly acquired information, to outline the alteration, and to identify the diagenetic minerals which can be attributed to the migration of hydrocarbons at the Cement-Chickasha oil fields. This petroleum originated in pre-Permian rocks and was transported through Pennsylvanian faults and along the unconformity at the base of the Permian section. The stable isotope geochemistry of carbon and oxygen from carbonate cement and the sulfur from the diagenetic pyrite will be related to the hydrocarbon migration and petroleum producing horizons at depth.

Study Area

The area of study is located in southwestern Oklahoma in Caddo and Grady Counties. The Cement Anticline was named after the town of Cement, which is near the center of the area of investigation. A large percentage of the study was focused in the area on or just off the flanks of the northwest- to southeast-trending structure. Respectively, Oklahoma City and Chickasha are approximately 50 and 9 miles northeast of the study area (Fig. 1).

Procedures

This investigation deals with the subsurface alteration at the Cement-Chickasha Anticlines. The many oil wells drilled in this area since its discovery made this possible. Drill cuttings were the main source of information as only one core of useful depth was available from the area. These cuttings and the core were obtained on loan from the Oklahoma Geological Survey Sample Library and the Shawnee Well Service.

Twenty-four wells were selected for the investigation (Table I).

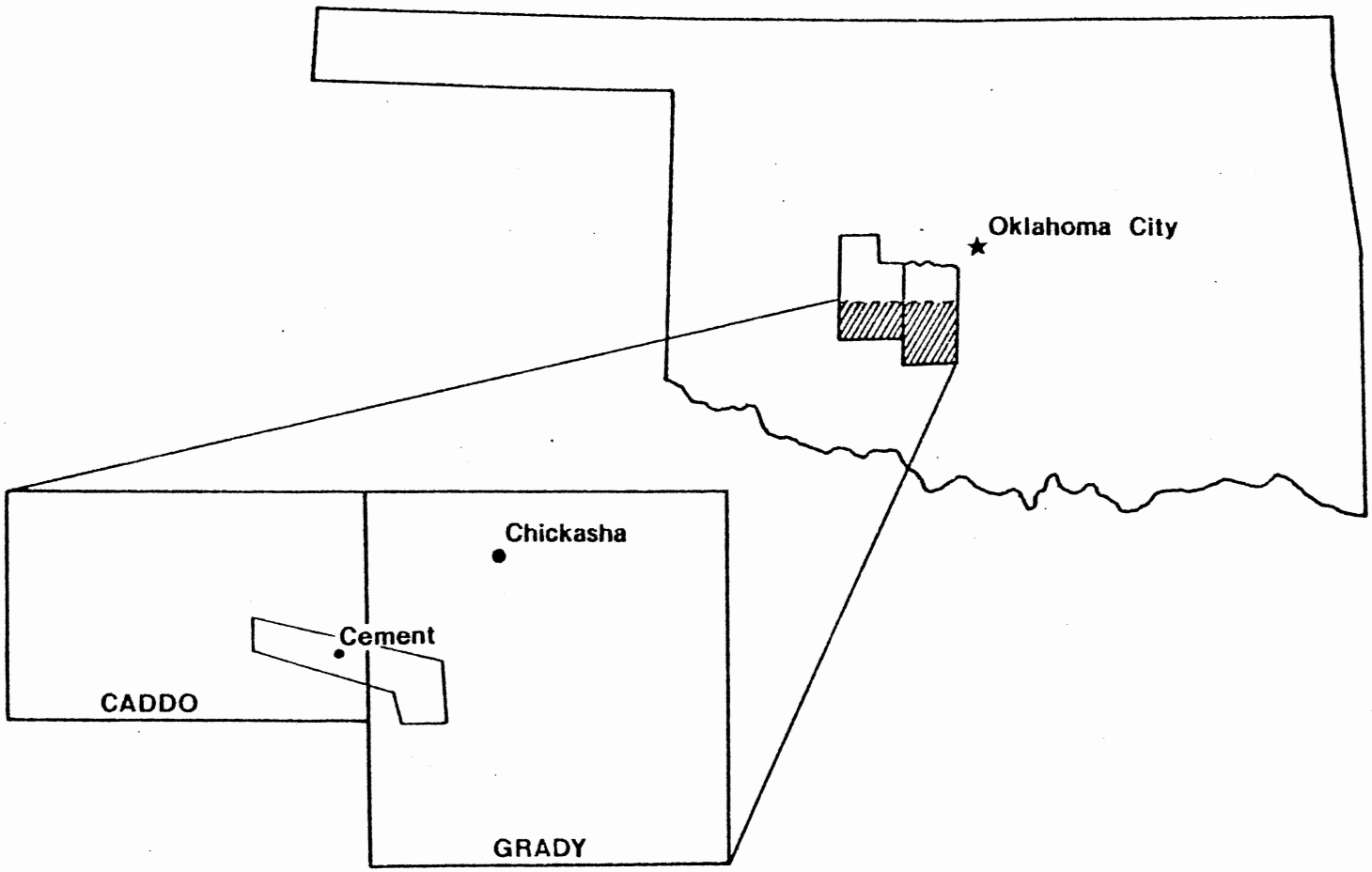

Fig. 1.--Index map of the study area (after Allen, 1980).

TABLE I

WELL LOCATIONS AND SAMPLE INTERVALS

	Well Number	Location	Interval Studied	Core/Cuttings
1.	Magnolia Petroleum Henley #2	NE,NE,SE 35-6N-10W	300'-2600'	all cuttings
2.	Midstates Oil Corp. Gray #2	SE,SE,SE 34-6N-9W	200'-2400'	all cuttings
3.	Amerada Petroleum W.J. Wood #1	NE,NE,SW 1-5N-10W	1900'-2900'	all cuttings
4.	Amerada Petroleum Hartshorne #1	NE,SE,NE 2-5N-10W	400'-2880'	all cuttings
5.	English Petroleum Kunsmuller #1	SE,SE,SW 32-6N-9W	500'-2520'	all cuttings
6.	Skelly Oil Williams B #1	SE,SE,NE 8-5N-8W	1000'-3000'	all cuttings
7.	Phillips Petroleum Thomas #1	NE,SW,NW 7-5N-8W	1000'-2100'	all cuttings
8.	Oklahoma Natural Gas Rider #1	NE,NE,SE 16-5N-8W	770-2210'	all cuttings
9.	Sun Oil Garret #1	C,SE,NW 21-5N-8W	300'-3000'	all cuttings
10.	Ohio Oil Hemphill #1	NE,NW,SW 18-5N-8W	500'-2900'	all cuttings
11.	Sinclair Oil Charleston #6	C,SW,SE 22-5N-8W	700'-2700'	all cuttings
12.	Carter Oil Smith #1	C,SE,SW 26-5N-8W	30'-2570'	all cuttings
13.	Ohio Oil Lemon#2	SW,SE,SE 2-5N-9W	200'-2500'	all cuttings
14.	Ohio Oil Kla-da-lug #3	NE,NW,NW 10-5N-9W	400'-600' 800'-900' 1100'-1200' 1500'-1600' 2100'-2300' 2400'-2600' 2700'-2800'	all cuttings many intervals missing

TABLE I (continued)

	Well Number	Location	Interval Studied	Core/Cuttings
15.	Ohio Oil Pau Kune #12	NW,SW,SE 3-5N-9W	2430'-2980'	all cuttings
16.	Ray Stephans Co. Melton #2	NE,SW,SE 26-6N-10W	1100'-3450'	all cuttings
17.	Oxley Petroleum	NE,NE,SW 5-5N-8W	200'-3280' (200'-1900') (1900'-2260') (2250'-2400') (2400'-2580') (2580'-3240') (3240'-3292')	 cuttings cored cuttings cored cuttings cored
18.	Caulkin's Oil Co. Youngblood #1	SE,SE,NE 15-6N-10W	1400'-2800'	all cuttings
19.	Trigg Oil Co. Smith #1	C,SE,NW	2100'-2600'	all cuttings
20.	Mack Oil Co. Shelnutt #1	NE,NW 19-6N-8W	2600'-3000'	all cuttings
21.	Frankfort Oil Co. Black-Bear #A-2	SE,NW,NE 9-5N-10W	1200'-2600'	all cuttings
22.	Johnson Heirs Olson #1	C	2000'-2680'	all cuttings
23.	Palmer Oil Corp. Davis #1	SE,SE,NE	3000'-3200'	all cuttings
24.	Phillips Petr. Co. Nicklos #1	C,NE,NE	2750'-2400'	all cuttings

Seventeen of these were on or near (within 1.5 miles) the crest of the structure. Seven wells served as control wells to determine the outer limits of the alteration, and were as far as five miles from the anticlinal axis.

The selection of these wells was based on surface alteration and availability of cuttings (i.e., location, absence of missing intervals, length of samples, and depth of samples), cores, and electric logs. The Oklahoma City Geological Society Log Library was the source of all electric logs used.

The well cuttings were examined with a binocular microscope and described in detail. Lithologic sections representing 39,800 feet of cuttings and cores were constructed placing emphasis on lithology, texture, color, and evidence of diagenetic mineralization (i.e., carbonate, pyrite, etc.). Electric logs were used during the description as a lithology guide and reference to insure correct depths.

Numerous photographs of the core were taken showing the diagenetic features.

Samples of the core were analyzed by a Phillips X-ray diffraction machine to determine the clay mineralogy. Bulk samples and clay extractions were analyzed to find overall mineral percentages and to identify the clay fractions, respectively.

Several samples in each well were subjected to detailed petrographic analysis. These thin sections were made by Central Petrographic Service, Inc., Dallas, Texas. Blue epoxy was impregnated into the pore spaces to show porosity and permeability. The thin sections were stained with alizarin red to identify the calcite cement and potassium ferrous cyanide to distinguish the iron-bearing carbonates. Several photomicrographs were

taken of the more obvious diagenetic mineral relationships.

Several samples were examined using a scanning electron microscope for the identification of diagenetic minerals.

Throughout the description of the cuttings, samples of diagenetic pyrite and carbonate minerals were selected for isotopic analysis. These subsurface samples provided 29 δS^{34} values from pyrite and 20 δO^{18} and δC^{13} values from carbonates. Two surface samples containing pyrite and three containing carbonate were also analyzed. Two gypsum samples taken from the surface were analyzed for δS^{34} content. Six crude oil samples were taken from Permian and Pennsylvanian producing horizons and analyzed for δS^{34} and δC^{13}. Histograms were constructed to show the frequency distribution of δC^{13}, δO^{18}, and δS^{34} of the carbonate and pyrite samples. Figures were also made to show the distribution of each of the isotopic δ values in the stratigraphic sections studied. All isotopic samples in this study were analyzed commercially by Geochron Laboratories, Cambridge, Mass.

Using parts of the data described above, five cross sections were constructed (Plates 1, 2 and 3). These cross sections were built using electric logs, lithologies, abundance of diagenetic minerals, and isotopic information. They were designed to show the diagenetic imprints of each stratigraphic zone and their lateral and vertical extent in the subsurface. Additional isotopic information from Donovan (1972) were also plotted in the appropriate stratigraphic positions. These cross sections are: AA', BB', CC', DD', and EE' (Fig. 2).

AA' runs in an east-west direction and is the longest cross section, based on information obtained from the ten wells that cut across the east and west Domes and run parallel to the north end of the Chickasha Anticline.

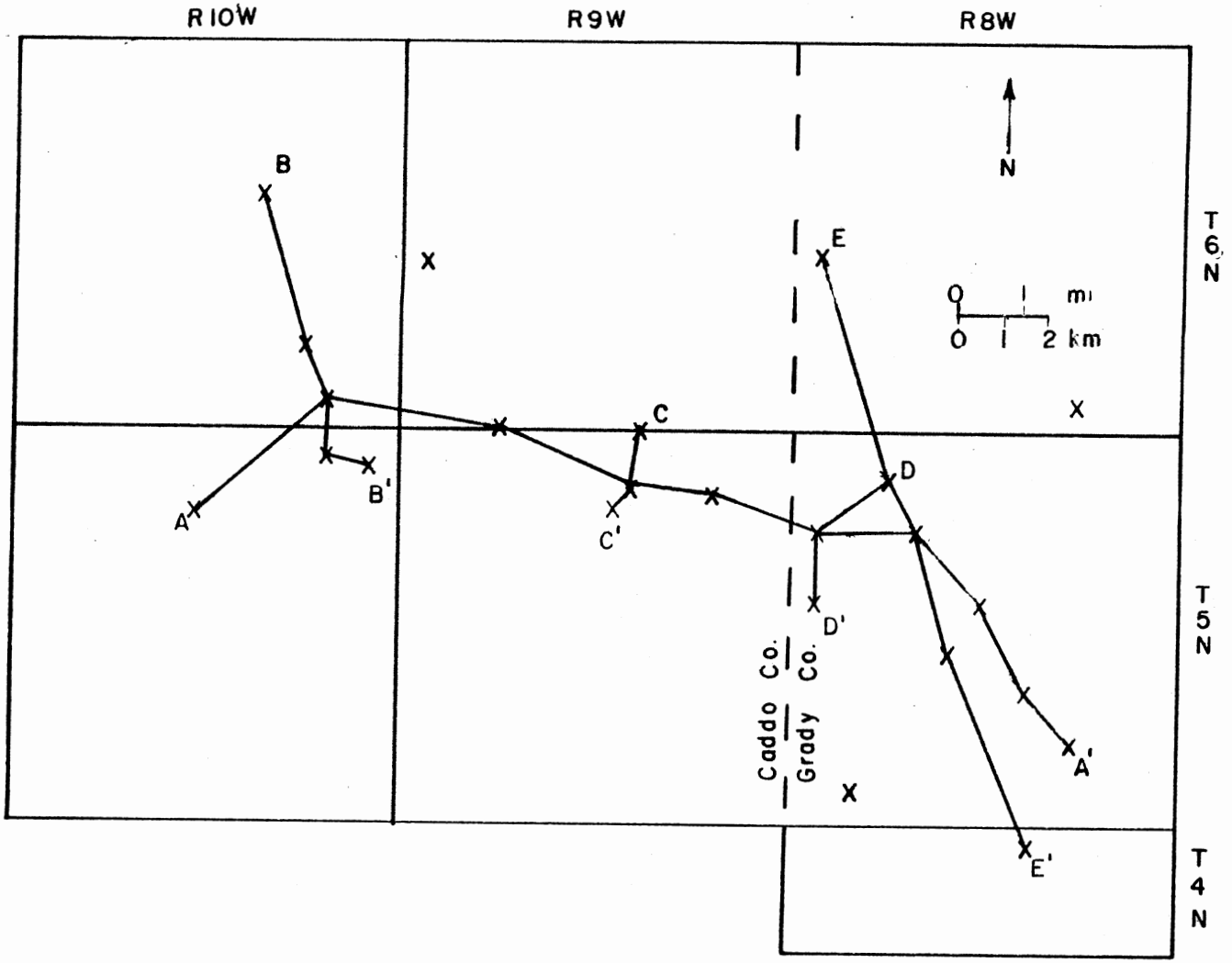

Fig. 2.--Location of wells studied (X) and cross sections.

BB' is a north-south cross section located in the western part of the study area, and cuts across the West Cement Dome.

CC' is a north-south cross section which takes in the East Cement Dome.

DD' and EE' are also north-south cross sections that provide information on the east end of the study area which includes the Chickasha oil field.

Each cross section contains the following information:

1. Lithologic description based on well cuttings examination.
2. Spontaneous potential and resistivity curves from electric logs.
3. Percentages of pyrite and carbonates, from examination with binocular microscope; additional qualitative explanation found in the legend of each cross section.
4. Location and depth of isotopic analysis of samples and their corresponding values.
5. Location and depth of samples selected for detailed petrographic anlaysis.
6. Location and depth of native sulfur occurrences.
7. Structure of the area.

CHAPTER II

GEOLOGICAL SETTING

The major emphasis of this chapter is placed on Permian red beds in south-central and southwestern Oklahoma. Near the town of Cement the Permian strata are approximately 3000 feet thick and range in age from Wolfcampian to Lower Guadalupian. In southern Oklahoma these beds are a series of fine-grained, friable, reddish-brown sandstones, and red siltstones and shales. At the Cement and Chickasha anticlines, the gently folded Permian beds lie unconformably above the Pennsylvanian Cisco Group. The pre-Permian units are more intensely folded and faulted than the strata above them.

The most striking characteristic of the study area is the high degree of alteration of the red beds which is observed on outcrops and to a considerable depth. These beds have become highly cemented with carbonates and pyrite, and have experienced color changes from red to green, buff or white.

Regional Tectonic Setting

The study area is located approximately 20 miles northeast of the eastern block of the Wichita Mountain uplift, in the eastern end of the Anadarko Basin (Fig. 3).

The Anadarko Basin trends northwesterly and is separated from the Wichita Mountain uplift by a zone of high angle reverse faults 10 to 20

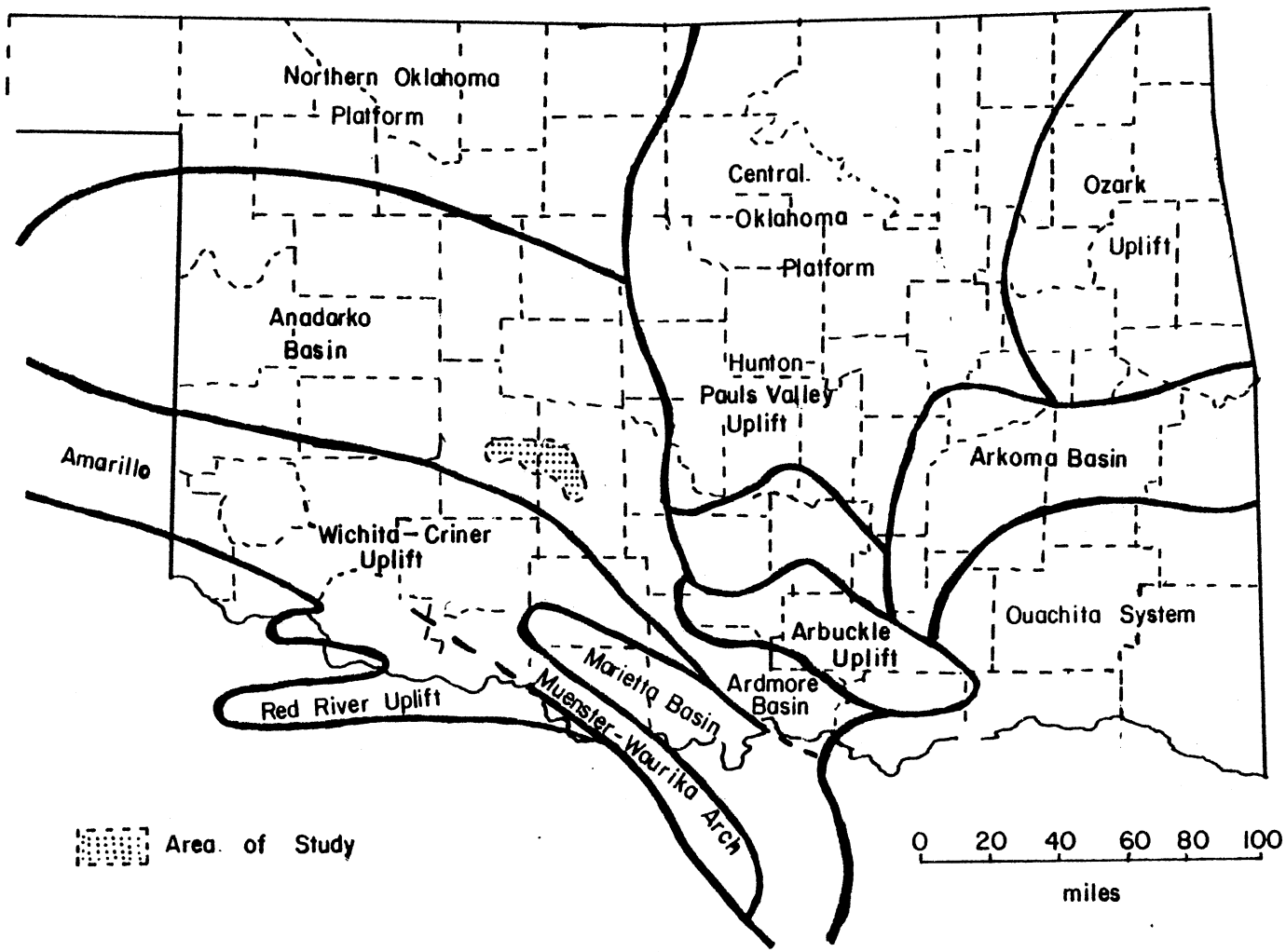

Fig. 3.--Major geologic provinces (Al-Shaieb, Shelton, and others, 1977).

kilometers wide (Ferguson, 1974). This basin was formed originally as part of the Southern Oklahoma Aulacogen, which was a prominent negative feature throughout much of the Paleozoic Era.

Wickham and others (1975) described three stages of structural development within the Southern Oklahoma Aualcogen: (1) The rifting stage (Latest Precambrian through Middle Cambrian) during which extensional normal faulting and the extrusion and emplacement of both mafic and felsic igneous rocks resulted in the early aulacogen as a graben with an igneous flooring. The majority of these rocks were from a subalkaline silicic magma (Hanson and Al-Shaieb, 1980); (2) The subsidence stage (Late Cambrian through Early Devonian) was marked by an initial marine transgression and the deposition of 10,000 feet of carbonate sequence with interbedded shale and sandstone units; (3) The deformational stage (Late Devonian through Early Permian) was concordant with the formation of the Ouachita orogenic system. During this phase subsidence in the basin and uplift of positive features was followed by rapid sedimentation.

The uplifting of the Wichita Mountains Complex began in Early Pennsylvanian time and ended in the Wolfcampian stage of the Permian Period. At the core of this complex are mafic and felsic rocks of Cambrian age that are related to the basement rocks of the Anadarko Basin. The uplift extends in the subsurface into Texas where it is called the Amarillo uplift.

By Early Permian time most tectonic activity in the area had ceased, except for minor folding of Permian units over older Pennsylvanian structures.

Local Tectonic Setting

The Cement Anticlinal Trend is subparallel to the trend of the Anadarko Basin and runs in a west-northwesterly direction. Along its crest this trend is expressed as a topographic high dominated by two domes, the East and West Cement Domes, separated by about four miles. The East Cement Dome has a closure in surface strata of about 60 feet while the West Cement Dome closure is about 140 feet (Donovan, 1974). This anticline is approximately 11 miles long and 2 miles wide and has, on the surface at the crest, Permian rocks dipping from 1° to 3° (Reeves, 1922). The unfaulted Permian section unconformably overlies faulted and tightly folded structures ranging in age from Pennsylvanian to at least Mississippian. The Permian beds are gently folded into a slightly asymmetrical anticline that has an increasing asymmetry with depth. The northeast flank of the structure is more steeply dipping, reflecting a major south-dipping reverse fault at depth; it is, therefore, downthrown on the north side. The fold axis and a north-dipping normal fault system parallels this reverse fault on the south. This normal fault has a variable throw and is substantially larger at the West Dome than the East Cement Dome. Several minor normal faults occur at an angle to the major faults at both domes (Fig. 4). All faulting appears to be pre-Permian and is truncated by the unconformity at the top of the Pennsylvanian.

The Chickasha anticline, which is located about five miles east-southeast of the town of Cement, trends north-northwest and is about five miles long and two miles wide (Fig. 4). Its axis runs parallel to the Chickasha fault, a high-angle reverse fault (Herrmann, 1961). The Chickasha anticline and the Cement anticline seem to converge somewhere in

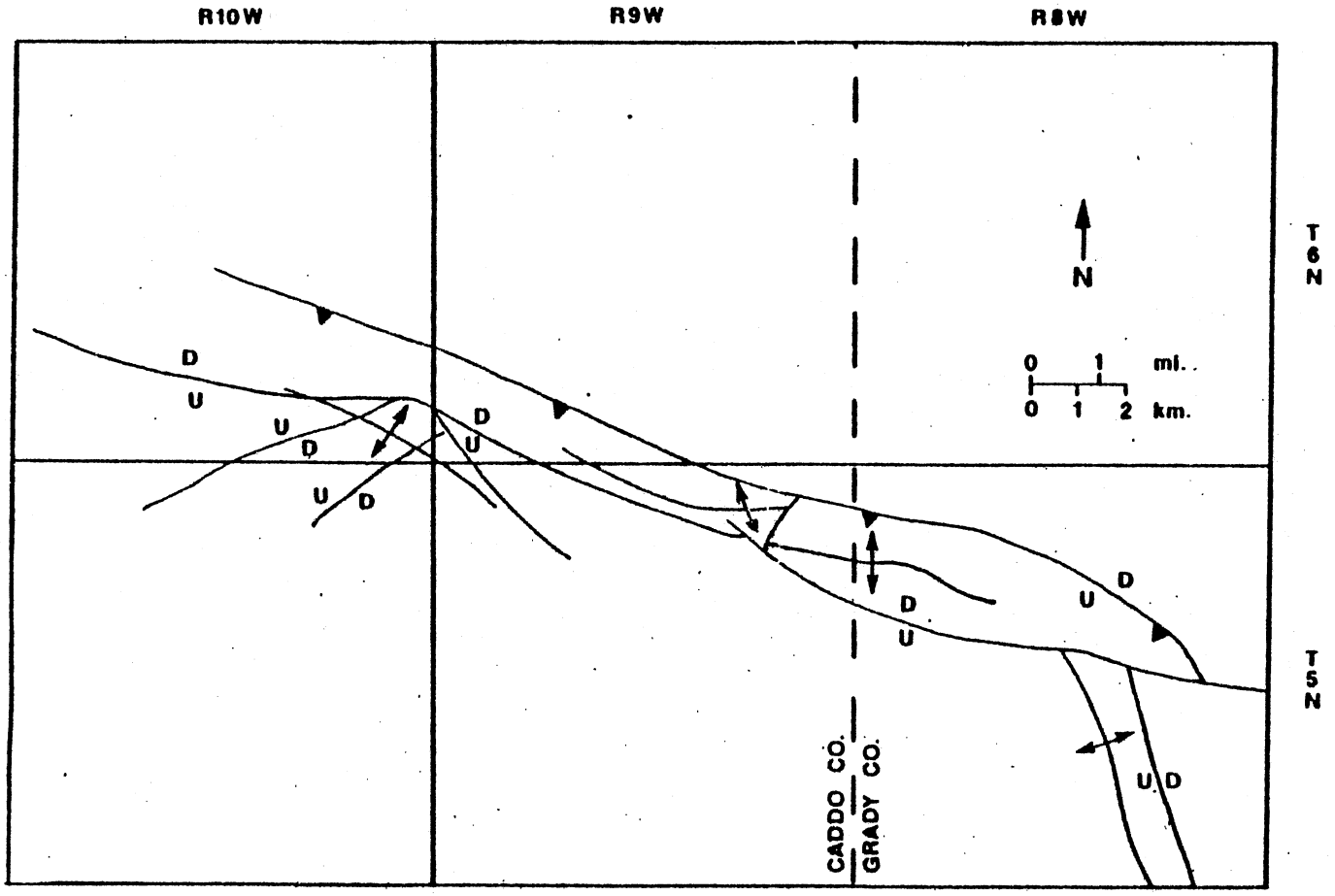

Fig. 4.--Pre-Permian structure (after Allen, 1980).

sections 15 or 16 of T. 5N., R. 8W.

The deformation that produced the Cement structure appears to have begun in Early Pennsylvanian. Rocks aging from Morrowan up to the unconformity at the base of the Permian show marked thinning over the crests of the structures indicating continued structural growth during this period (Herrmann, 1961). As further supportive evidence, sedimentary units thicken on the downthrown side of major faults indicating deposition concurrent with structural development (Herrmann, 1961).

Stratigraphic Setting

Only the Permian section was studied in this investigation because alteration is confined to rocks of this age. Below is a brief description of these formations as taken from the literature, and as they appeared in the drill samples described during this study.

Wolfcampian Series

The Oklahoma Geological Society recognizes nomenclature for the Lower Permian of southwest Oklahoma that has not received broad acceptance or usage. They claim the Permian begins at the base of the Wellington Formation in the Cimarronian Series. This study uses the more widely accepted nomenclature which recognizes the Pontotoc Formation of the Wolfcampian Series as basal Permian. Figure 5 shows a stratigraphic section of the study area and the equivalent units according to the Oklahoma Geological Society.

Pontotoc Group

The Pontotoc Group is extremely heterogeneous and does not show

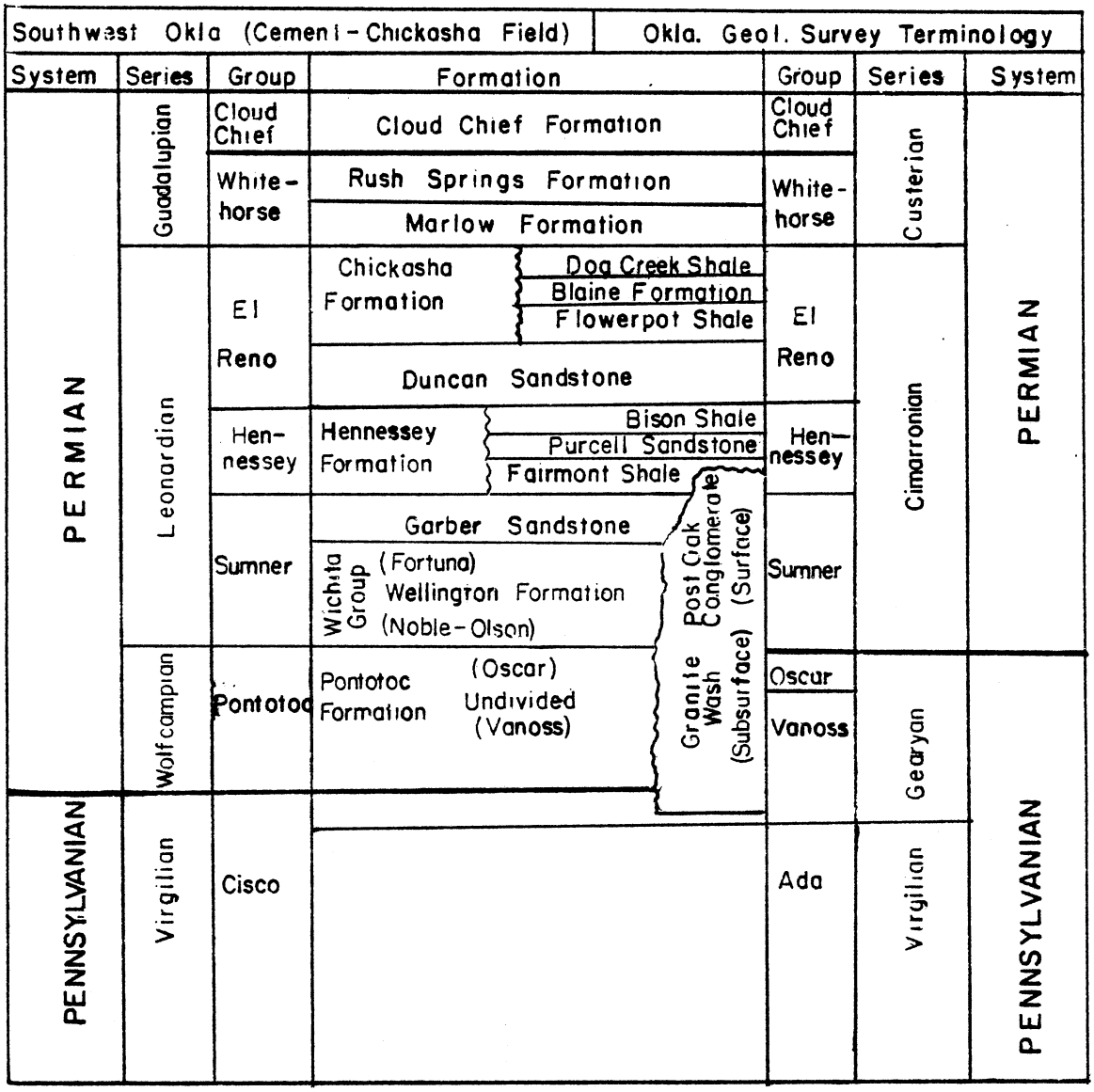

Fig. 5.--Columnar section for southwest Oklahoma (modified from Miser, 1954; Herrman, 1961; Thomas, 1981; Harlton, 1960).

natural subdivisions.

Pontotoc Formation. Permian sedimentation began with the Pontotoc Formation. At Cement the Pontotoc rests unconformably on the highly truncated Pennsylvanian Cisco beds. These beds are almost wholly detrital in origin. They typically consist of alternating deep maroon shales, locally arkosic, and intercalated cherty, arkosic, sandy conglomeratic limestones and fine- to coarse-grained sandstones (Harlton, 1960). The top of the unit is marked by a silty, sandy, oolitic limestone of variable thickness, which was found in only one well in the area.

Leonardian Series

The Sumner Group, The Hennessey Group, and the El Reno Group make up the Leonardian Units in south-central Oklahoma.

Sumner Group

This group includes the Wellington Formation and the overlying Garber Sandstone (Fig. 5).

Wellington Formation. The Wellington Formation is a series of interbedded shales and sandstone units that range from black or brown massively bedded (up to 50 feet thick), to well-cemented, thin-bedded units of yellow, gray, or black fine-grained sandstones. The remainder of the Wellington Formation is predominantly red shales and local sandstone lenses.

The shales and sandstones of the Wellington Formation in the Cement-Chickasha areas are unevenly altered to green and accompanied by

disseminated pyrite cubes and calcite filling pores and fractures. Very coarse sand to pebbles of carbonate are common throughout the formation. Several layers of calcite nodules also occur in the lower half of the red shale unit. These nodules are commonly scattered but occasionally they coalesce to form a bed as a calcrete deposit.

Since the oolitic limestone marking the top of the Pontotoc was found in only one well, the exact boundary between the Wellington Formation and the Pontotoc Formation was not easily determined. For this study the boundary was picked at a point approximately 50 to 100 feet below the Noble Olson sands in the base of the Wellington Formation on the basis of a study by Harlton (1960).

Garber Sandstone. Usually, the sandstone members of the Garber Sandstone are thin, hard, reddish-brown, gray, or black with cross bedding (Dott, 1930), but massive lenses occur locally. Its reddish-brown color distinguishes it from the older Permian rocks. Bunn (1930) described the basal member, the Asphaltum Sandstone Bed, as a buff to gray, massive- to thin-bedded, calcareous sandstone, generally friable and medium grained, which is locally asphaltic. This bed ranges in thickness from 20 to 50 feet. Bunn (1930) and Munn (1914) described carbonate conglomerates in some areas in addition to shale units that divide the sandstone members.

In the study area this formation has an approximate total thickness of 200 feet, is usually altered to variegated green and red, and contains disseminated pyrite and calcite cement. In some specific intervals this unit is completely green in color with pyrite content exceeding 25 percent.

Hennessey Group

The Fairmont Shale, the Purcell Sandstone, and the Bison Shale comprise the Hennessey Group in western Oklahoma. In the study area they are undifferentiated and are known collectively as the Hennessey Formation. Interfingering with this shale near the Wichita Mountain Uplift is its coarse distal stratigraphic equivalent, the Post Oak Conglomerate (Allen, 1980) (Fig. 5).

Hennessey Shale. The Hennessey Shale is commonly silty and ranges from gray to reddish-brown in color. Fine-grained, light tan sandstone lenses occur locally, as do pink to white thin beds of gypsum. The shales of this formation are commonly blocky and calcareous. In the study area the shale is commonly spotted to massively altered to green in color, and pyrite is common throughout the unit with some 10-foot drilling sample intervals containing as much as 50 percent pyrite. The thickness of the Hennessey Shale is variable, and in the Cement area it ranges from approximatley 450 to 750 feet.

Fay (1968) describes the Post Oak Conglomerate as stratigraphically equivalent to the Hennessey Shale. Miser (1954), however, considers it equal to the upper part of the Wichita Formation which is older than the Hennessey Shale. The Post Oak Conglomerate is a granite boulder conglomerate adjacent to the Wichita Mountains and with distance grades into a gravel facies, and finally an arkose and arkosic sandstone interfinger with the Hennessey Shale (Chase, 1954; Ferguson, 1977). Significant amounts of sandstones and mudstones occur within the unit and the name Post Oak Formation was preferred by Al-Shaieb and others (1979).

El Reno Group

The El Reno Group consists of the Duncan Sandstone and the Chickasha Formation (Gould, 1924). The Dog Creek Shale, the Blaine Formation, and the Flower Pot Shale are lateral stratigraphic equivalents to the Chickasha Formation but are not developed in the study area (Fig. 5).

Duncan Sandstone. The Duncan Sandstone consists of two to three massive, buff to gray-green, fine to very fine-grained sandstones with dolomitic lenses (Self, 1966). Siltstones and shales occur throughout the formation with a general coarsening-upward sequence, resulting in its topmost units being conglomeratic and cherty. In the study area where the approximate thickness of the Duncan Sandstone is 250 feet, disseminated pyrite and calcareous cement is common.

Chickasha Formation. The Chickasha Formation, which ranges from 200 to 300 feet in thickness, is characterized by sandstones, siltstones, shales and maroon gypsiferous mudstones containing coarse to very coarse sandstone grains. The sandstones and shales in the study area commonly contain carbonate cements and pyrite and are variegated in color.

Where the Chickasha Formation grades into the Dog Creek Shale and the Blaine Formation north of the study area, the section consists of red, blocky, silty shales, interbedded with fine-grained gypsiferous sandstones and locally pure gypsum (Davis, 1955).

Whitehorse Group

The Whitehorse Group contains the Marlow Formation and the overlying Rush Springs Formation (Fig. 5). These are mainly fine-grained sandstones and siltstones with occasional thin dolomite and gypsum beds.

Marlow Formation. The Marlow Formation consists of fine-grained sandstones and gypsiferous, silty shales of reddish-brown color. Satin-spar gypsum prevails throughout the unit. The Verden Sandstone Member occurs near the middle of the unit and consists of a light brown, lenticular, medium- to coarse-grained sandstone, characterized by thick beds and calcium carbonate cement. In the upper part of the section, two thin dolomite beds are separated by a red sandstone and shale unit of about 16 feet. In the study area, the formation is about 120 feet thick and is commonly green to white and contains some pyrite and calcite cement.

Rush Springs Formation. The Rush Springs Formation is a light brown to reddish-brown, even to highly cross bedded, friable, silty sandstone. The generally fine-grained, quartzose sandstone has moderate amounts of hematite and clay minerals as cement. Siltstones and shales are not common in this formation.

In this study area, the approximate 250-foot section of the Rush Springs Formation is highly altered. This unit is normally a red friable sandstone, but on outcrop over the Cement Anticline it is a buff to white highly cemented sandstone. This cement is mostly calcium carbonate but some pyrite is present in small nodules (1 inch across). In some areas on the structure, a hydrocarbon odor can be detected from a freshly broken surface sample.

The Weatherford Gypsum Bed is a massive pink gypsum located in the upper part of the Rush Springs Formation. This gypsum bed ranges from 1 to 40 feet in thickness and is dolomitic with local variations to anhydrite (Davis and Tonaka, 1963). The Weatherford Gypsum Bed is separated by the overlying Cloud Chief Formation by 10 to 15 feet of dolomitic sandstone and siltstone.

Guadalupian Series

The Cloud Chief Group is the only Guadalupian age rocks present in this study area (Fig. 5).

Cloud Chief Group

The interbedded gypsum and red shale of the Cloud Chief Formation is exposed at Cement on the surface as several outliers.

Cloud Chief Formation. The Cloud Chief Formation contains 60 to 120 feet of basal gypsum and dolomite, overlain by approximately 300 feet of shale, siltstone, and sandstone. Within the study area only a small portion of the basal gypsum has been preserved. This gypsum, the Moccasin Creek Gypsum Member, is characterized by massive pink to white layers which contain a few sandstone layers.

At Cement, toward the crest of the structure, the gypsum grades into mixed gypsum and carbonate and at the top of the "Keechie Hills" the $CaSO_4$ of the gypsum has been completely replaced by $CaCO_3$. The result of this substitution is a resistive limestone with perfectly preserved gypsum crystal outlines.

Depositional Environment

Marine, marginal marine, and fluvio-deltaic were the major types of depositional environments that contributed to the sedimentary record of the Permian section of southern Oklahoma (Davis, 1955) (Fig. 6).

During Permian time the basins in southern Oklahoma were sites of deposition; the Anadarko Basin continued to subside under its sediment load. Fay (1964) named the Wichita Mountains as a major source of

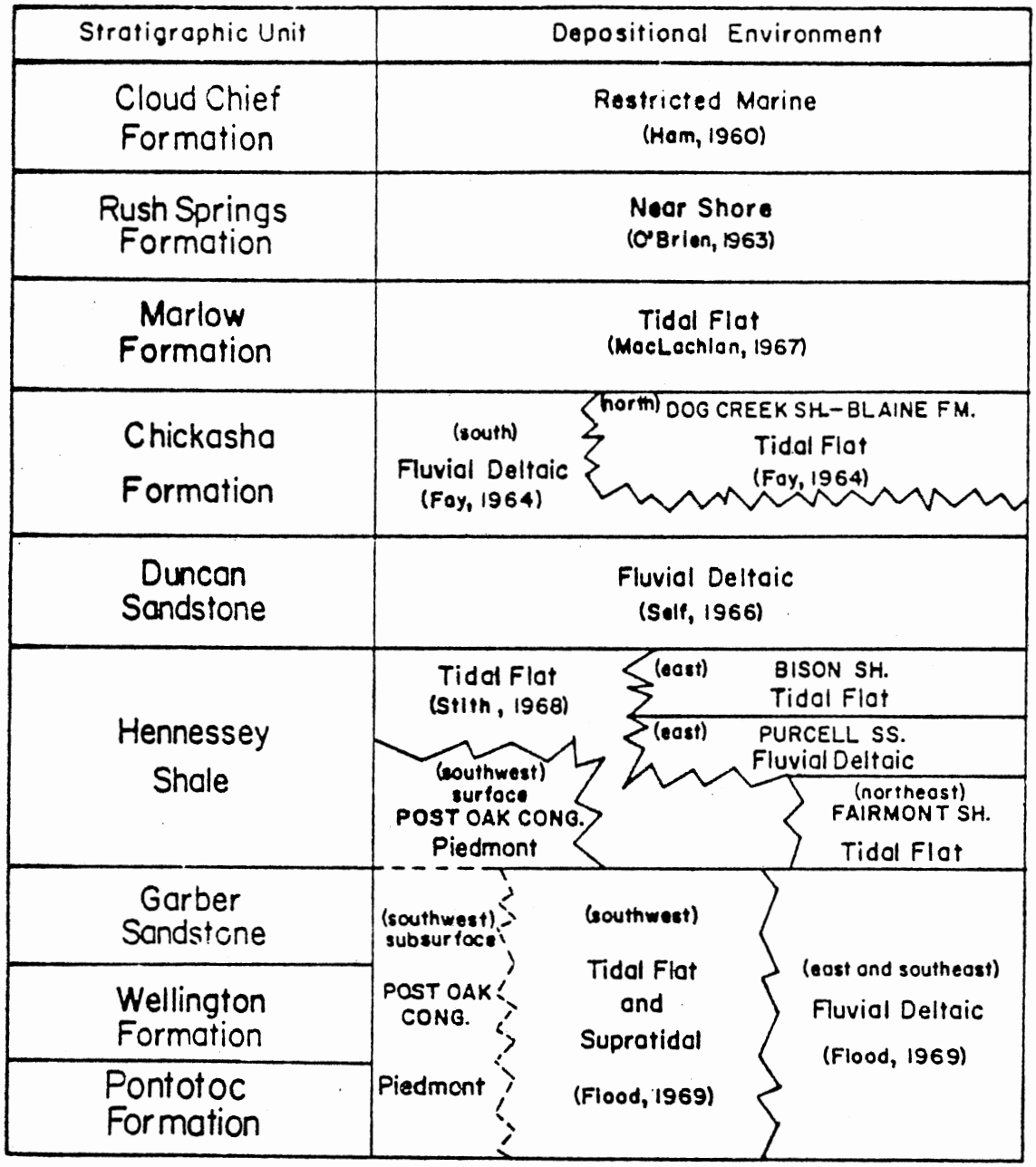

Fig. 6.--Stratigraphic unit and equivalent depositional environments, south-central Oklahoma (after Olmsted, 1975).

clastic detritus in this basin, but the Ouachita Mountains provided an increasingly important source during Early Leonardian time and throughout the remaining part of the Permian System.

The sandstone lenses of western Jefferson County, Oklahoma, of Early Permian age have been described as having a fluvial origin with the surrounding siltstones and shales representing floodplain and deltaic deposits (Flood, 1969). The Lower Permian rocks of south-central Oklahoma are believed to represent a similar depositional environment as that proposed by Flood (1969). There is evidence of brief marine incursions. Alternating with these incursions were arid climatic conditions which resulted in the formation of the pedogenic calcite nodules and the more developed calcrete beds. Above these calcrete horizons the Wellington Formation, as well as the Garber Sandstone, and Hennessey Shale were deposited in a variety of marine-dominated environments including deltaic, shallow marine, tidal flat, and supratidal (Davis, 1955).

Fay (1964) believed a large river flowing northwestward from the Ouachita Mountains provided the clastic source for the fluvio-deltaic environment which deposited the Duncan Sandstone and Chickasha Formation.

A shallow sea transgressed over the subsiding Chickasha Formation delta resulting in the deposition of the siltstones and sandstones of the Marlow Formation. This environment has been interpreted as brackish water to shallow marine (Fay, 1964) and as a tidal flat (MacLachlan, 1967).

With the continued uplifting of the Ouachita Mountains and its role as sediment source, the Rush Springs Formation was deposited in a shallow marine bay (Davis, 1955). These sands were exposed periodically by sea level fluctuations and were reworked into eolian dunes; probably as

coastal dunes (MacLachlan, 1967). Some deposits may have formed as strandline deposits (O'Brien, 1963). Coastal plain playa lakes or brackish backshore lagoons were represented by the siltstones and shales within the formation, while the gypsum and dolomite beds may be coastal sabkha deposits (Allen, 1980).

The deposition of the Cloud Chief Formation was interpreted by Ham (1960) to have occurred in a restrictive marine environment. Evaporitic conditions took place in a semi-enclosed arm of a sea when minor transgressions introduced incursions of sulfate-rich waters.

CHAPTER III

PETROLOGY AND DIAGENESIS

Petrology, diagenesis, and paragenetic sequence of alteration events were investigated in the subsurface of Chickasha and Cement oil fields. More than 39,800 feet of strata were examined using electric logs, well cuttings, and cores.

Petrologic and diagenetic information used in this chapter were provided by several analytical techniques and procedures. These include the scanning electron microscope (SEM), detailed petrographic analysis using stained thin sections, binocular microscope, carbon, oxygen, and sulfur isotope studies, and X-ray diffraction of bulk samples and extracted clay fraction.

The data collected during the course of this investigation were used to construct several cross sections (Plates 1, 2 and 3). These were based on well log, petrologic, diagenetic, and isotopic information. They are designed to show the diagenetic imprints of each stratigraphic zone and their lateral and vertical extent in the subsurface.

Mineralogical composition of various rock types was based on semi-quantitative X-ray diffraction analysis of 33 samples from the Wellington Formation. In addition, detailed petrographic analysis of 43 thin sections was performed on samples representing all rock types in the study area. The results of these analyses are listed in Table II.

General Lithologies

The rocks studied consist of claystone, shale, siltstone, sandstone, pebble conglomerates, and gypsum. Shales and claystones are the most abundant within the sections studied, totaling approximately 50 percent of the rock types. Siltstones and conglomerates are least abundant, constituting about 10 percent and 5 percent, respectively. Fine-grained sandstones make up the remainder of the samples. Gypsum beds occur at the surface and in the shallow subsurface. Irregular carbonate pebble conglomerates occur in the Wellington and Pontotoc Formations. Erratic, very coarse-grained sand is present in samples from the Marlow Formation through the Duncan Sandstone.

Along the structure the shales are variegated green and red with the intensity of alteration varying from well to well. Shales in close proximity to the permeable sandstones are more commonly green in color, although some random green mottling was found in thick shale sequences (Fig. 7). Green shale also occurs locally in association with the carbonate conglomerates (Fig. 8). The large majority of siltstones and sandstones on the structure are green in color, while few remain red. Some brown hydrocarbon-stained sandstones are also noted.

Alteration of red beds off the structure is not common. Most units retain their characteristic red stain, with only the most permeable sandstones being altered. When shales off the structure show alteration, it appears as small green spots.

Detrital Constituents

Quartz, feldspars, and carbonates comprise the three basic detrital minerals of the sediments (Fig. 9, Table II).

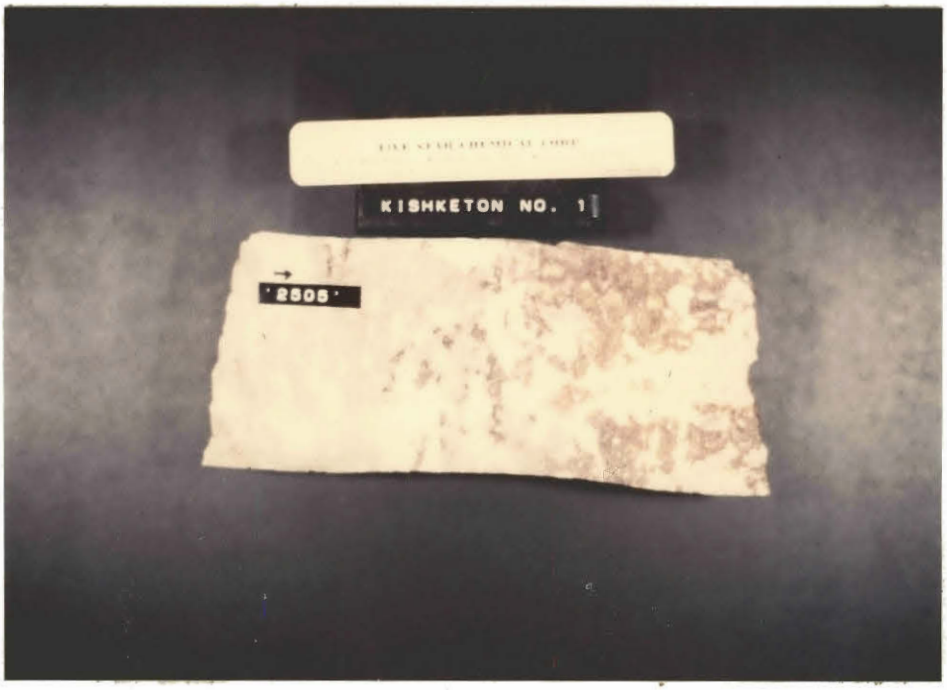

Fig. 7.--Photograph of green discoloration inside red shale unit.

Fig. 8.--Photograph of carbonate conglomerate in green shale.

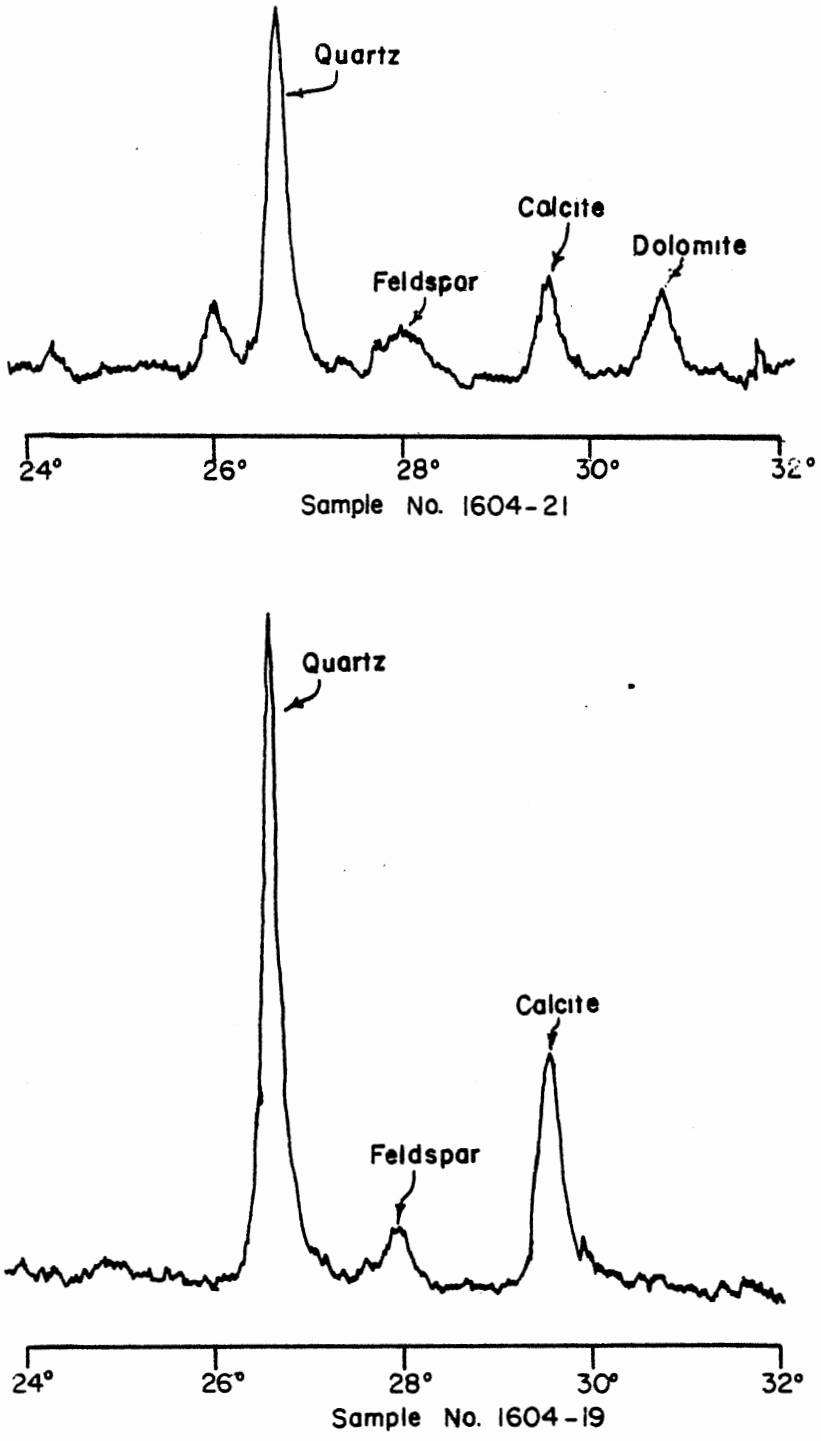

Fig. 9.--X-ray diffraction analysis for samples 1604-21 and 1604-19.

TABLE II

COMPOSITION OF SANDSTONES IN THE CEMENT AND CHICKASHA OIL FIELDS

Sample Number	Method of Determination	Qtz	Carbonates		Other	Feldspars	Clays	Pyrite
			Cement	Clasts				
2323-W1	Thin section	41	43	6	--	---	---	---
2080-G1	Thin section	70	30	---	--	---	---	---
4170-G1	Thin section	58	37	---	--	---	trace	5
3106-D1	Thin section	58	20	---	18 opal	trace	---	4
3106-G1	Thin section	63	24	---	10 opal	3	trace	trace
4481-G1	Thin section	90	6	---	5 opal	---	---	trace
4481-H1	Thin section	80	20	---	--	---	trace	trace
3065-H1	Thin section	90	10	---	--	---	---	---
3065-G1	Thin section	70	30	---	--	---	trace	---
3065-W1	Thin section	49	51	trace	--	---	---	---
2910-H1	Thin section	77	23	---	--	---	---	---
2910-RS1	Thin section	65	35	---	--	---	trace	---
2910-G1	Thin section	81	19	---	--	---	trace	---
4806-D1	Thin section	65	35	---	--	---	---	---
2278-D1	Thin section	64	24	---	--	---	---	1
4298-G1	Thin section	60	40	trace	--	---	---	trace
7163-G1	Thin section	60	40	---	--	---	---	---
4445-G1	Thin section	63	37	---	--	---	---	---
5013-G1	Thin section	67	23	---	--	---	---	10
4176-W1	Thin section	50	25	15	--	---	10	---
4176-G1	Thin section	74	21	---	--	---	---	5
1003-D1	Thin section	83	10	---	--	---	5	2
LQC-RS1	Thin section	80	15	---	--	---	---	5
ECP-RS1	Thin section	62	33	---	--	---	---	5

TABLE II (continued)

Sample Number	Method of Determination	Qtz	Carbonates		Other	Feldspars	Clays	Pyrite
			Cement	Clasts				
ECC-RS	Thin section	--	100	---	--	---	---	5
1604-A1	Thin section	60	40	---	--	---	---	---
1604-A2	Thin section	5	40	55	--	---	---	---
							Kaolinite/Illite	
1604-1	XRD	88	--	---	---	10	2	---
1604-2	XRD	80	12.5	---	---	7.5	---	---
1604-3	XRD	84	--	---	---	16	---	---
1604-6	XRD	66	17.5	---	---	8.5	8	---
1604-7	XRD	80	6.5	---	---	10.5	3	---
1604-8	XRD	77.5	--	---	---	11	3.5/8	---
1604-9	XRD	57	43	---	---	---	---	---
1604-10	XRD	65	14	---	---	21	---	---
1604-11	XRD	86.5	8.5	---	---	5	---	---
1604-12	XRD	89	--	---	---	9	2/<1	---
1604-13	XRD	81	--	---	---	13	6	---
1604-14	XRD	57	41	---	---	---	2	---
1604-15	XRD	81	--	---	---	17	2	---
1604-16	XRD	78	--	---	---	12	4/6	---
1604-17	XRD	71	23	---	---	3	3	---
1604-18	XRD	70	11.5	---	---	18.5	---	---
1604-19	XRD	39	28	---	---	9	4/10	---
1604-20	XRD	78	--	---	---	14	3/5	---
1604-21	XRD	39	42	---	---	19	---	---
1604-22	XRD	78	--	---	---	16	6/<1	---
1604-23	XRD	76.5	9	---	---	8.5	6	---
1604-24	XRD	76.5	--	---	---	10	7.5/6	---
1604-25	XRD	39	54	---	---	4	3	---
1604-26	XRD	58	24	---	---	---	/18	---
1604-27	XRD	14	80	---	---	---	6	---

TABLE II (continued)

Sample Number	Method of Determination	Qtz	Carbonates		Other	Feldspars	Clays	Pyrite
			Cement	Clasts				
1604-28	XRD	21	79	---	---	---	---	---
1604-29	XRD	66	--	---	---	---	29/14	---
1604-30	XRD	78	--	---	---	11	5/6	---
1604-31	XRD	65	--	---	---	11	8.5/15.5	---
1604-32	XRD	64	--	---	---	13	7.5/15.5	---
1604-34	XRD	81	--	---	---	16	8/6	---
1604-35	XRD	78	--	---	---	17	5/21	---
1604-36	XRD	78	9	---	---	10	3	---
Averages		66%	23%		.5%	5%	4%	.5%

Note: Letter after sample number denotes that sample's formation: RS = Rush Springs Formation; D = Duncan Sandstone; H = Hennessey Formation; G = Garber Sandstone; W or A = Wellington Formation. All samples whose percentages were determined with the XRD were from the Wellington Formation.

Quartz is the most abundant detrital grain in the study area (Fig. 9). This mineral makes up approximately 66 percent of the rocks. It is found in the sandstones mostly as fine, subangular to subrounded sand grains. Some very coarse sand grains are common in the Marlow through Duncan Sandstone. Silt and clay-sized particles are also present in the shale throughout the section. In the Rush Springs Formation, some of this quartz appears as frosted grains.

Feldspars are common in these rocks and can range up to 21 percent (Fig. 9, Table II) with the average being 5 percent. Several kinds are present including orthoclase, microcline and some plagioclase. They are present in thin sections throughout the stratigraphic units studied.

Dark gray to brown carbonate grains are common in the Wellington Formation. These grains range in size from very coarse sand to pebble. As mentioned earlier, they do not always show distinct bedding, and sometimes appeared to be dumped into an area during rapid sedimentation. Only two fossil fragments were found in the rocks studied. These fragments possibly had the same source rock as the detrital carbonate grains.

Large rip-up clasts of claystone were observed in a core from the Wellington Formation. These clasts are angular and randomly oriented indicating deposition in a high energy environment (Fig. 10). The X-ray diffractograms indicate an increase in clay matrix in beds containing the clasts. The majority of sandstones have relatively small amounts to no detrital clay matrix. The most common detrital clay is illite.

Rock fragments and chert are also present throughout the section studied. Although the rock fragments are common, they compose a very small percentage of the total rocks. The chert is even less common.

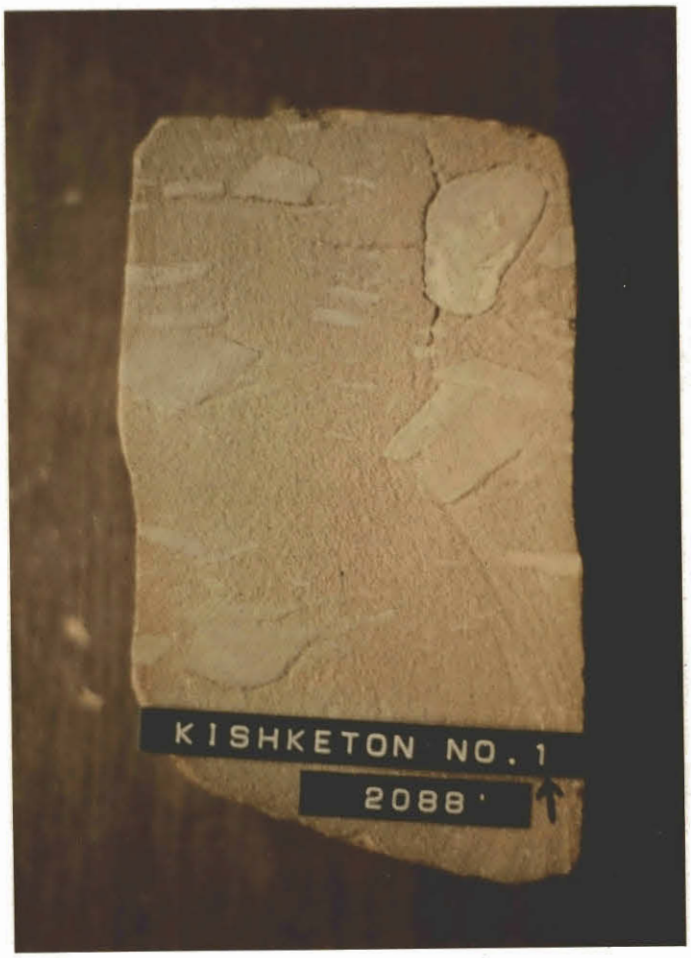

Fig. 10.--Photograph of clay ripup clasts in sandstone.

Fig. 11.--Photograph of wood fragments from the Pontotoc Formation.

Carbonized wood fragments and coal is present in the Wellington and Pontotoc Formations (Fig. 11). Slabbed cores exhibit some woody cellular structure still intact.

Diagenetic Constituents

The most striking feature of the Cement-Chickasha Anticline is the extreme amounts of diagenetic alteration present in the rocks. The obvious color change (from red to green, buff, and yellow) on the surface was first recorded by Reeves (1922). He reported the color change with carbonate mineralization present over the structure. With more recent studies, including this one, it has been found that pyrite, clays, magnetite, and gypsum are commonly important diagenetic minerals in addition to carbonates. These minerals extend into the subsurface at least to the unconformity at the base of the Permian.

Pyrite

Pyrite is found in all stratigraphic units in the study area except the Cloud Chief Formation. It is present as either cementing nodules (Fig. 12 and 13) or as small disseminated cubes (Fig. 14). Marcasite occurs as a minor constituent. In the subsurface pyrite is present in the green colored units and is commonly accompanied by the occurrence of free sulfur. On outcrop it also appears as small veinlets. The nodules are present in the Rush Springs Formation as small holes pitting the surface with a limonite stain trailing downward (Fig. 15). This results from oxidation of pyrite to iron oxide and hydroxide. Unaltered pyrite nodules, however, can be found within one inch of the rock surface (Fig. 12). Large portions of the wood fragments in the Wellington

Fig. 12.--Photograph of cementing pyrite nodules from a surface sample.

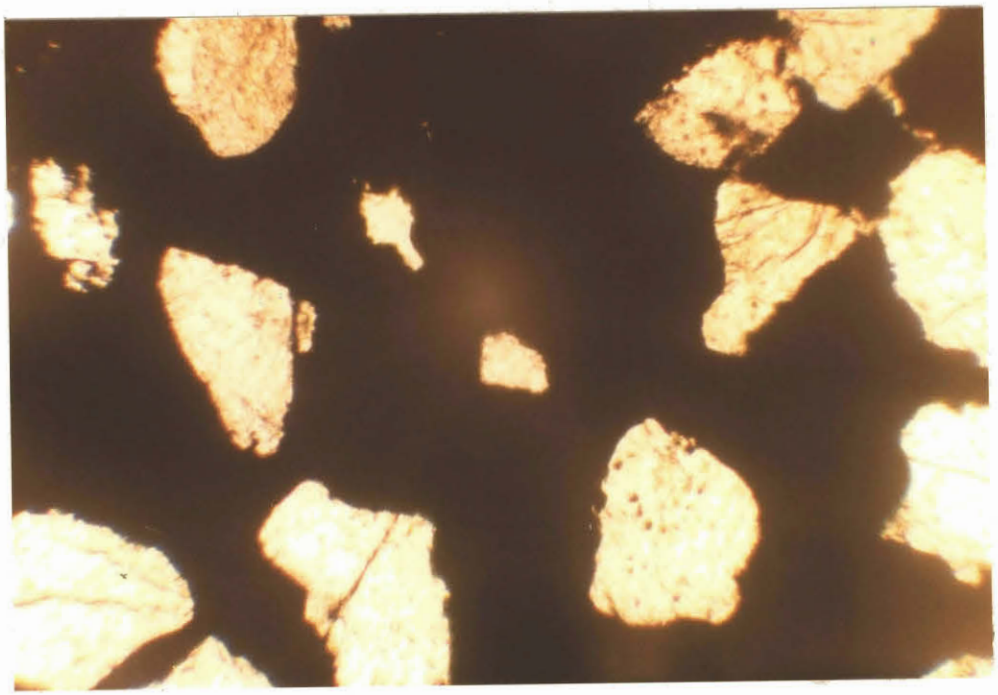

Fig. 13.--Photomicrograph of pyrite cement showing corrosion of detrital quartz grains.

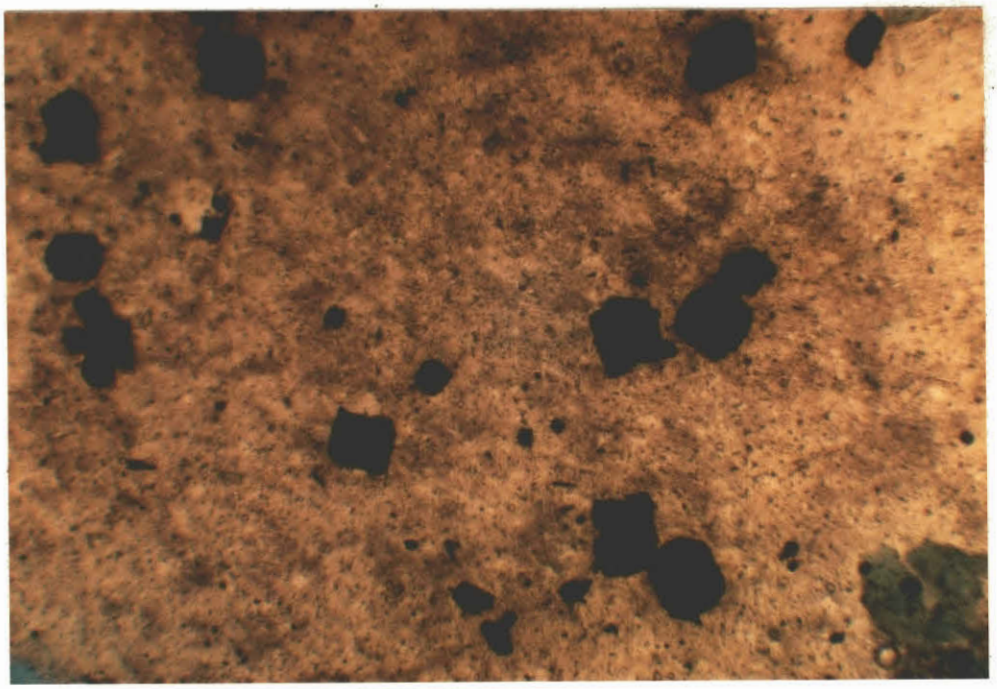

Fig. 14.--Photomicrograph of disseminated pyrite cubes in shale.

Fig. 15.--Photograph of pyrite nodule weathering to limonite on outcrop.

Formation were replaced by pyrite. (This pyrite formed by bacterial reduction, as it is explained later, and is not necessarily the same age as the disseminated pyrite.)

Ferguson (1977) also reported diagenetic pyrite in the Velma, Eola, and Chickasha Oil Fields.

Using Eh-pH diagrams, Ferguson (1977), following Donovan (1972), showed that the formation of pyrite in red beds could be the result of reduction of hematite by the H_2S gas associated with hydrocarbons. In this process the iron is changed from the ferric to ferrous state with the sulfur in pyrite provided by the gas (Kartsev and others, 1959):

$$2H_2S + Fe_2O_3 \rightarrow FeS_2 + FeO + 2H_2O \quad (1)$$

Donovan (1972) thought that the ferrous iron was being transported away in the migrating fluids. The free sulfur close to the pyrite cubes is the result of the oxidation of the H_2S (Davis and Kirkland, 1970):

$$H_2S + \tfrac{1}{2}O_2 \rightarrow S^o + H_2O \quad (2)$$

Carbonate Cement

Carbonate cement is also very common (Table III). Most sandstones throughout the section studied contain some of this cement. The Rush Springs Formation contains such a large amount of carbonates it has been quarried at both East and West Cement Domes for road materials and is referred to as a "limestone". When this "limestone" is freshly broken a hydrocarbon odor is given off. Donovan (1972) used this fact and the presence of solid hydrocarbons around grains to conclude the hydrocarbon migration preceded carbonate mineralization. Lesser amounts of carbonates occur in some shales. By use of alizarin red and potassium ferrous cyanide it can be shown that the carbonates consist of both calcite and

TABLE III

PERCENTAGES OF CARBONATE CEMENTS IN THIN SECTIONS
COLLECTIONS FROM CEMENT AND
CHICKASHA OIL FIELDS

Well Name	Sample Number	Total % CO_3 Cement	Percent and Type Carbonate
Pau Kune #12	2323-W1	43	43% calcite
W. J. Wood #1	G-2080-G1	30	30% ferroan dolomite
Kunesmuller #1	A-4170-G1	37	37% calcite
Hartshorne #1	H-3106-D1	20	20% calcite
Hartshorne #1	H-3106-G1	24	20% calcite, 4% ferroan dolomite
Charleston #6	A-4481-G1	6	3% calcite, 3% ferroan dolomite
Charleston #6	A-4481-H1	20	20% calcite
Melton #2	A-3065-H1	10	8% dolomite, 2% ferroan dolomite
Melton #2	A-3065-G1	30	30% calcite
Melton #2	A-3065-W1	51	30% ferroan dolomite, 20% dolomite, 1% calcite
Smith #1	A-2910-RS1	30	22% dolomite, 5% ferroan dolomite, 3% calcite
Smith #1	A-2910-H1	23	23% calcite
Smith #1	A-2910-G1	19	12% calcite, 7% ferroan dolomite
Gray #2	F-4806-D1	35	30% calcite, 5% dolomite
Lemon #2	C-2278-D1	25	15% ferroan dolomite, 10% calcite
Rider #1	A-4298-G1	40	37% ferroan dolomite, 3% calcite
Garret #1	F-7163-G1	40	40% ferroan dolomite
Williams B#1	F-4445-G1	37	35% ferroan dolomite, 2% calcite
Thomas #1	F-5013-G1	23	20% ferroan dolomite, 3% ferroan calcite
Henley #2	A-4176-G1	21	21% ferroan dolomite
Henley #2	A-4176-W1	25	25% calcite
Hemphill #1	A-1003-D1	10	10% calcite
Kishketon #1	1604-A1	40	40% calcite
Kishketon #1	1604-A2	40	40% calcite
Surface	LQC-RS1	15	15% calcite
Surface	ECP-RS1	33	33% calcite
Surface	ECC-RS	100	100% calcite

Note: Letter after sample number denotes that sample's formation: RS = Rush Springs Formation; D = Duncan Sandstone; H = Hennessey Formation; G = Garber Sandstone; W or A = Wellington Formation.

dolomite, which are locally iron-bearing (Fig. 16 and 17).

The precipitation and dissolution of calcite is explained by the following equations:

$$CaCO_3 + H_2CO_3 \leftrightharpoons 2HCO_3^- + Ca^{++} \quad (3)$$

$$CO_2 + H_2O \leftrightharpoons H_2CO_3 \quad (4)$$

The CO_2 is evolved from the oxidation of hydrocarbons during its migration toward the surface. The ferroan nature of carbonates is explained by the incorporation of Fe^{++} ions in the carbonate lattice to produce ferroan calcite and/or dolomite by the following reactions:

$$CaCO_3 + xFe^{++} \leftrightharpoons (Ca_{1-x}, Fe_x)\ CO_3 + xCa^{++} \quad (5)$$

Ferroan Calcite

$$4CaCO_3 + Fe^{++} + Mg^{++} \leftrightharpoons 2Ca\ Fe_{.5}\ Mg_{.5}\ (CO_3)_2 + 2Ca^{++} \quad (6)$$

Ferroan Dolomite

The Fe^{++} ions represent a byproduct of the reduction of Fe^{3+} (in hematite) during hydrocarbon migration. Therefore, Fe^{++} is very abundant in formational waters.

Authigenic Clay Minerals

Authigenic clays were identified by scanning electron microscope and X-ray diffraction techniques (Fig. 18). The SEM showed abundant kaolinite booklets, and some mixed-layer illite-smectite (Fig. 19). The delicate projections on these clays indicate clearly they are authigenic. The X-ray diffraction analysis also showed kaolinite being the most abundant authigenic clay (Fig. 18). Pore filling kaolinite was observed in thin section. Based on a broad peak on the X-ray diffractogram, illite is the major detrital clay mineral in the Permian red beds in the study area. Therefore, it is assumed that the diagenetic reactions related to

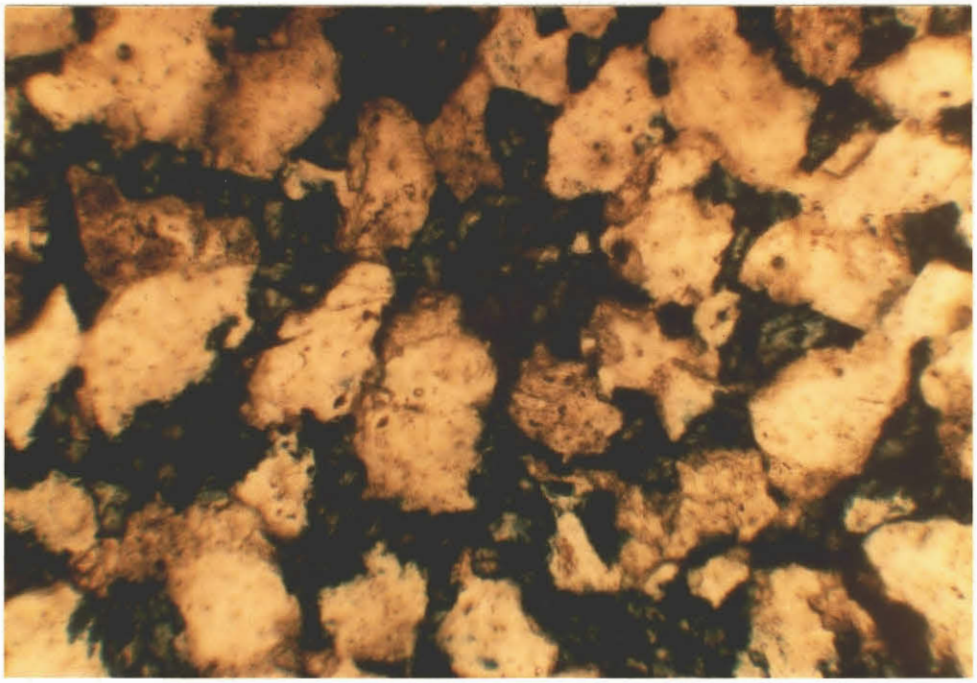

Fig. 16.--Photomicrograph of ferroan dolomite cement in sandstone.

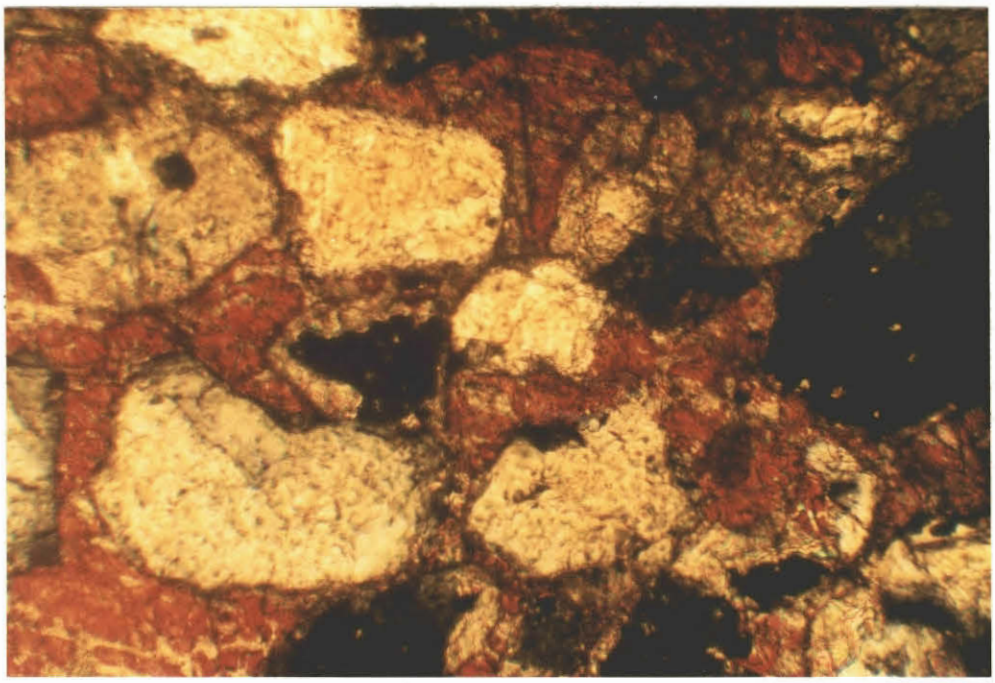

Fig. 17.--Photomicrograph of calcite cement and dolomite replacing quartz grains.

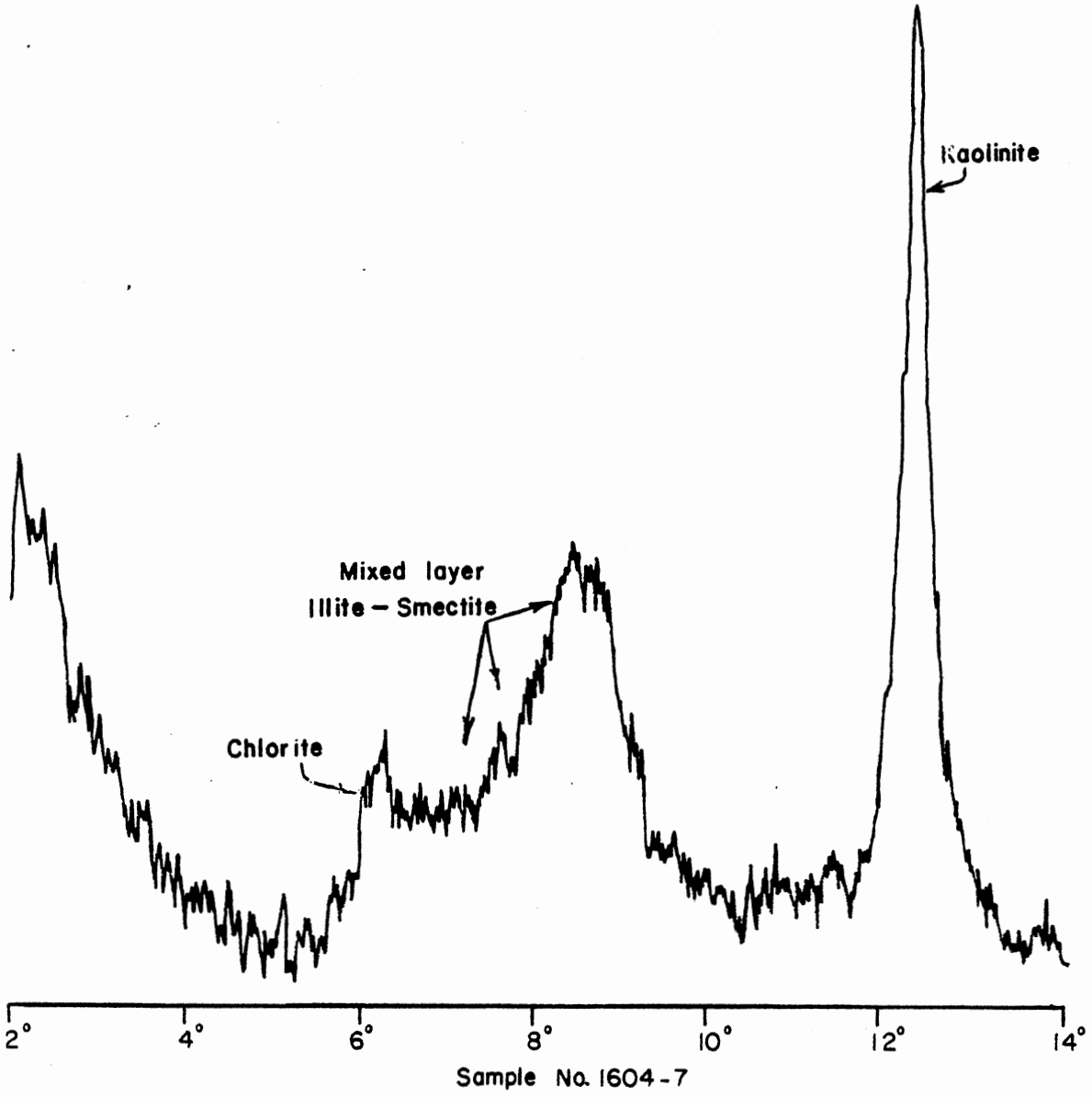

Fig. 18.--X-ray diffraction analysis of clay fraction from sample 1604-7.

Fig. 19.--SEM photograph of authigenic kaolinite booklets and mixed-layer illite-smectite.

hydrocarbon migration reflect drastic changes in the chemistry of the formation water. As a result, illite became unstable under the new equilibrium conditions and authigenic kaolinite and illite-smectite mixed layer clays were formed. The following equations may explain the transformation of detrital feldspar and illite to kaolinite and smectite, respectively:

$$\underset{\text{K-Feldspar}}{2KAlSi_3O_8} + 2H^+ + 9H_2O \rightleftharpoons \underset{\text{Kaolinite}}{H_4Al_2Si_2O_9} + 2K^+ + 4H_4SiO_4 \quad (7)$$

$$\underset{\text{Mica}}{2KAl_3Si_3O_{10}(OH)_2} + 2H^+ + 3H_2O \rightleftharpoons \underset{\text{Kaolinite}}{3H_4Al_2Si_2O_9} + 2K^+ \quad (8)$$

Boles (1979) proposed the following reaction for the transformation of smectite to illite:

$$4.5\ K^+ + 8Al^{3+} + \underset{\text{Smectite}}{KNaCa_2Mg_4Fe_4Al_4Si_{38}O_{100}(OH)_{20}}\ 10H_2O \rightleftharpoons$$

$$\underset{\text{Illite}}{K5.5\ Mg_{12}Fe_{1.5}Al_{22}Si_{35}O_{100}(OH)_{20}} + Na^+ + 2Ca^{++} + 2.5FE^{+3} + 2Mg^{++} + 3Si^{4+} + 10H_2O \quad (9)$$

This reaction was based on Hower et al. (1976) model:

$$\text{Smectite} + Al^{+3} + K^+ \rightleftharpoons \text{Illite} + Si^{+4} \quad (10)$$

Also, the phase diagram in Figure 20 may also help explain this transformation.

Miscellaneous Diagenetic Products

Donovan, Forgey, and Roberts (1979) reported magnetic anomalies over the Cement Oil Field. They interpreted this "as reflecting abundant near-surface magnetite formed by the reduction of hydrated iron oxide and/or hematite as a direct result of petroleum microseepage"

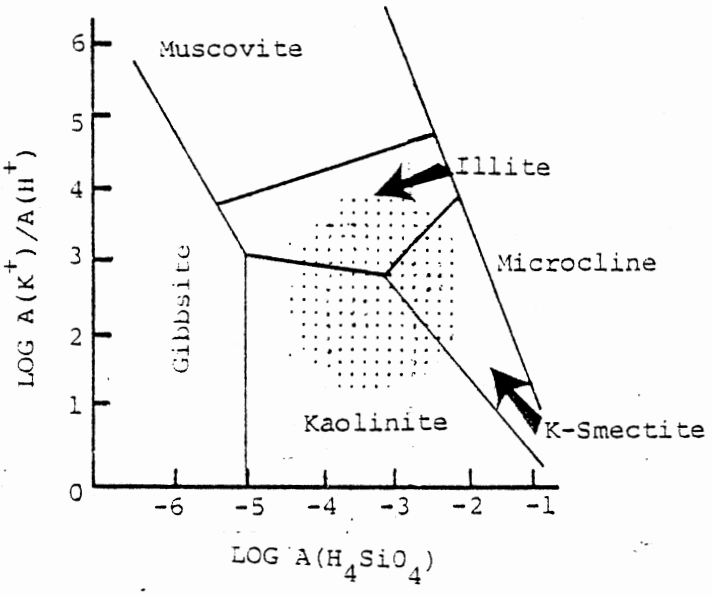

Fig. 20.--Stability field diagram for common minerals in K_2O-Al_2O_3-SiO_2-H_2O system (after Shvartsev and Bazhenov, 1978).

(Donovan, Forgey, and Roberts, 1979, p. 245). They proposed a sequence of alterations to take place as follows:

hydrated ferric oxides → hematite → magnetite

(Fe_2O_3) $(Fe^{2+} Fe_2^{+3} O_4)$

Syntaxial quartz overgrowths are not very common in the sandstones in this study area, although some are recognizable with the SEM.

Poikilitic gypsum-anhydrite cement in well samples is common in the sandstones from the surface downward to the Upper Hennessey Shale. It represents the downward percolation of sulfate-rich waters from the overlying Cloud Chief Formation.

Autochthonous Sediments

The main representative of the non-clastic sediments in the study area is gypsum. This gypsum forms thick beds in the Cloud Chief Formation that are exposed at the surface. Thinner fibrous beds of gypsum associated with occasional thin dolomites extend down through the section into the Upper Hennessey Shale.

Thin dolomite and limestone stringers are present in the sediments below the Garber Sandstone.

Diagenetic History and Paragenesis of Diagenetic Events

Thin section examination and scanning electron microscopy were the basis of most of the interpretation of the chronological sequence of diagenetic minerals (Fig. 21).

The initial formation of the hematite staining in the entire Permian section were penecontemporaneous with its deposition. The calcrete in

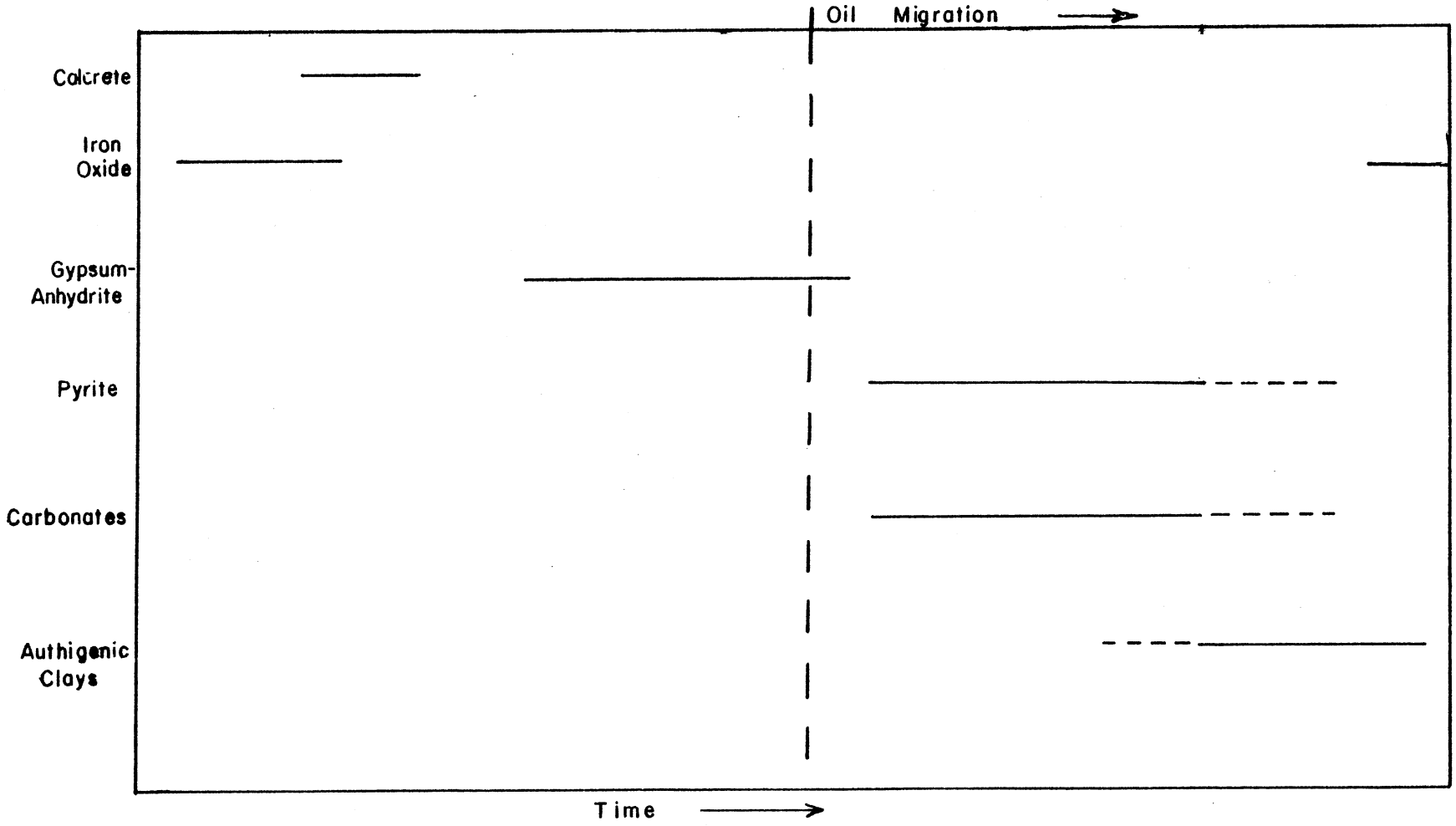

Fig. 21.--Paragenesis of diagenetic events.

the Wellington Formation began forming shortly after or during the time the rocks were stained red (Fig. 22).

The anhydrite-gypsum cement occurred later as a result of infiltration of sulfate-rich surface rocks.

Hydrocarbon migration appears to have occurred either during the period of anhydrite cementation or shortly after. With this migration the hydrocarbons supplied the H_2S and, through reactions, HCO_3^- that resulted in the formation of the pyrite and carbonate cements, respectively.

The kaolinite and illite-smectite mixed-layer clays formed as late stage diagenetic pore fillings and pore bridging clays reflecting changes of pore water conditions.

The final alteration was the reoxidation of the iron in the pyrite cement exposed on the surface. In this reaction the iron is converted to its ferric form resulting in the limonite on the surface exposure.

Surface Alterations

The surface alterations at the Cement field resulted in friable Permian red beds being altered to highly cemented green and buff sandstones. It has been mapped on color alone from aerial photographs (Donovan, 1972). Also, Allen (1980) did field mapping by a combination of color and occurrence of diagenetic minerals.

The color change and mineralization has been found to cut across bedding planes, especially where they pinch out down the flanks of the structure. Sparry calcite and lesser amounts of dolomite cement these surface rocks. Generally, maximum mineralization occurs at the crest of the anticline making the top of the structure more erosion resistant than the less mineralized rocks on the flanks. The result is a pronounced but

Fig. 22.--Photograph of calcrete deposit from the Wellington Formation.

irregular topographic relief.

Allen (1980) mapped six diagenetic zones. Zone one is the "normal" Rush Springs Formation that is unaltered, friable, and hematite stained. Zone two is designated as unaltered Rush Springs Sandstone with hematite spotting. Zone three includes a color change to buff or yellow from a limonite staining. There is no carbonate present in this zone. Zone four resembles zone three except for the presence of sparry calcium carbonate cement. This cement comprises 30 percent of the rock. Zone five consists of "limestone" (sandstone of the Rush Springs Formation which is very highly cemented with carbonate) containing concretions or small veinlets of pyrite. Zone six is the "limestone" with no pyrite.

The alteration and replacement of gypsum by calcite also occurred at the crest of the East and West Cement Dome. This replacement was caused by the oxidation of sulfates by the migrating hydrocarbons resulting in perfect preservation of the gypsum crystals as calcite.

Subsurface Alteration

Cross sections constructed from electric logs, lithologic logs, diagenetic mineral abundance, and isotopic information were used to interpret the diagenetic imprints on various stratigraphic units (Plates 1, 2 and 3).

The diagenetic mineral percentages shown in these plates were based on microscope examination of well cuttings from ten-foot intervals.

The occurrence of diagenetic pyrite in shale is localized, whereas the pyrite content generally is consistent throughout the sandstone unit. However, a decrease in pyrite is observed with depths in the wells on the structural flanks. A higher percentage of pyrite is present over

the anticlinal axis and domes. This amount decreases on the flanks and away from the structure where the pyrite mineralization is absent within 2.5 miles. The Hennessey Shale locally contains large amounts of pyrite (up to 50 percent), whereas all sandstones more consistently contain as much as 20 percent pyrite. Wells on the upthrown side of Pennsylvanian faults, located between the anticlinal axis and faults, tend to have a larger amount of pyrite throughout the section compatible with the idea that pyrite formed from H_2S associated with hydrocarbon migrating up through the pre-Permian faults. This gas then seems to have moved updip and permeated stratigraphic units. Thick green shale sections containing pyrite supports crosscutting of stratigraphic units by H_2S.

Free sulfur occurs more frequently in sandstone, is observed in all stratigraphic units, and follows no recognizable structural or stratigraphic trends.

The occurrence of diagenetic carbonate in shale units is localized, but the carbonate cement content in most sandstones is evenly distributed throughout the individual unit, although exceptions do occur. This may be a direct result of good porosity and permeability giving precipitating fluids easy access to lateral movement. Therefore, most permeable sandstones (located on the structure or its near flanks) have some carbonate cement. The amount of carbonate cement decreases gradually away from the structure until it is uncommon to absent in wells three to five miles away.

Correlation between the amounts of pyrite and carbonate cements in an interval is generally very good. This can be attributed to the similar conditions that resulted in their precipitation (i.e., permeable beds in close proximity to a structural trap to which hydrocarbon by-products have access).

CHAPTER IV

MIGRATION, ACCUMULATION, AND ALTERATION OF HYDROCARBONS AT THE CEMENT-CHICKASHA OIL FIELD

Donovan (1972) used physical and chemical properties of crude oil and diagenetic carbonate cements to trace the migration of hydrocarbons at the Cement Oil Field. Ferguson (1977) demonstrated this migration could also be traced by the distribution of diagenetic pyrite cement. Both investigators felt the theory of petroleum migration presented by Baker (1969) best explained their observations.

From his study of hydrocarbon-solubility data, Donovan (1974) found that the log of activity coefficients of different hydrocarbons varies with salt concentration. These activity rates depend on the type of hydrocarbon and salt. He suggested that aromatic compounds exsolve with increasing NaCl concentrations at faster rates than n-paraffin. Donovan (1974) also suggested that a selective dissolution of low-molecular-weight hydrocarbon components resulted with salinity changes in migrating formation waters.

Partial evaporation of crude oils involves the selective loss of dissolved gases and then the lighter oil fractions. This leaves an enrichment of heavy fractions in the remaining entrapped oil. All crude oils at the Cement Oil Field have gravities ranging from 32-36° API, except the Marchand crude from the south flank of the East Cement Dome. The latter crude largely has an API gravity range of 10-18°, which

suggests that the Marchand is the source of the massive, long-term leakage of hydrocarbons responsible for the alterations at the surface. Donovan (1974) indicated the Marchand zone also has low-gas volume, and anomalous isotopic and chemical compositions which indicate fractionation and loss of more mobile hydrocarbon constituents. Donovan (1977) described one seepage mechanism as the effusion of gaseous and liquid hydrocarbons through relatively thin overburden along faults and fractures and through poorly compacted and permeable caprocks.

A synopsis of the migration, and accumulation of oils, and subsequent alteration of overlying beds at the Cement-Chickasha fields involves several steps. Initially, hydrocarbons were generated and accumulated in pore spaces within shales. With increased pore pressure they began migrating upward and outward from the deepest part of the Anadarko Basin and accumulated in anticlinal structures. Migration and accumulation of petroleum was during and after the structural deformation of the study area (Ferguson, 1977). Microseepage of petroleum from the Marchand sands was principally along the pre-Permian faults. This possibly could have formed surface seepage during Pennsylvanian time. The Permian was unconformably deposited over the Pennsylvanian; the resulting unconformity truncated the fault system which it intersected at the crest of the Cement-Chickasha Anticlines providing means for the migration and accumulation of leaking petroleum into Permian strata. This process resulted not only in accumulations in Permian reservoirs, but also in the alterations throughout the Permian section. Two main alterations occurred; the oxidation of hydrocarbons produced a carbonate cement, whereas H_2S associated with petroleum reduced iron oxide and formed pyrite.

CHAPTER V

ISOTOPIC COMPOSITION

Since the discovery of deuterium by Urey (1932), great advances have been made in the study of isotopes. In the last 25 years, much work has been done on the various isotopes related to hydrocarbons. This chapter will deal with the S^{34}, C^{13}, and the O^{18} isotopes from diagenetic minerals in the Cement-Chickasha Oil Field and how they relate to the hydrocarbon migration.

Sulfur Isotopes

Theory

Thode et al. (1958) set the basic framework for working with sulfur isotope data in crude oils. Since then there has been considerable research dealing with the sulfur in the petroleum, its associated H_2S gas, and the SO_4 in gypsums and ground water.

The sulfur isotope data is expressed in terms of the quantity δ, which is defined by the S^{34}/S^{32} abundance ratio in the sample compared to the standard ratio in the troilite of the Canon Diablo meteorite:

$$S^{34} = \frac{[S^{34}/S^{32}]\ \text{Sample}}{[S^{34}/S^{32}]\ \text{Standard}} - 1 \quad \times 1000$$

with the values reported in per mil (0/00). When the δ is positive the sample is said to be heavy because it contains a larger relative amount of S^{34} than the standard.

The δS^{34} of crude oils has a relatively narrow range, as compared to the terrestrial biogenic sulfur compounds. The δS^{34} range for particular oil pools is much smaller. Thode and Monster (1965) reported an apparent relationship in the δS^{34} values between gypsum-anhydrite deposits and the petroleum sulfur of the same age. They found a 15‰ displacement in the δS^{34} content, Vrendenburgh and Cheney (1971) supported the relationship but claimed the difference to be 20‰ for unaltered oils (Fig. 23). These observations have been used as evidence that sulfur in petroleum is derived from a bacterial reduction of sea-water sulfate trapped within the source rock.

Thode, Monster, and Dunford (1958), Thode and Monster (1965), and Thode and Monster (1970), presented evidence that indicated stability of the sulfur isotope during the process of maturation. But such an interpretation has not always proven to be applicable. Cheney (1964) found sulfur isotopic modification resulted from petroleum maturation, this is supported by the studies of Vrendenburgh and Cheney, (1971), and Orr, (1974). Maturation results in fractionation which increases the δS^{34} values. As the maturation proceeds, the δS^{34} content of the oil continues to increase, and at temperatures greater than 80° - 120°C it approaches the value of sulfate of the same age (Orr, 1974).

The mechanism that increases δS^{34} may be related to the associated H_2S gas (Orr, 1974). In his study, Orr found that the H_2S was constantly slightly heavier than the oil, while during maturation the oil itself becomes increasingly heavy. This led him to believe these increases were due to competing sulfurization processes, and to propose two kinetically-controlled processes working in opposition: the release of free sulfur from the reduction of sulfate by hydrogen sulfide, and oxidation of hydrocarbons with the sulfur to give more hydrogen sulfide

and carbon dioxide.

In their early work, Thode et al. (1958) indicated that there was very little difference in the δS^{34} values of petroleum and associated H_2S. Other studies (Thode and Monster, 1965; Vrendenburgh and Cheney, 1971; Orr, 1974), however, have shown that the δS^{34} contents of H_2S and its oil can differ slightly. On the average the H_2S has been found to be enriched in δS^{34} by approximately 2‰ (Krouse, 1977).

Goldhaber (1978) constructed a histogram, from published δS^{34} data of H_2S associated with petroleum. His results show a range of +10 to -15‰ with a skewness to the positive side (Fig. 24).

There are examples in the literature that show similar δ values for sulfur in pyrite and their associated bituments (Harrison and Thode, 1958) and where the δ values show a similar trend in a basin (Krouse, 1977).

Ferguson (1977) suggested H_2S gas was reducing the iron oxide, in the red beds of his study area, to produce pyrite. This H_2S had its source with buried hydrocarbons and was transported along faults and an unconformity.

Goldhaber, Reynolds, and Rye (1978), and Reynolds and Goldhaber (1978) present evidence of iron sulfide forming diagenetically from fault-derived H_2S associated with oil and gas reservoirs at depth. They also documented an increase of sulfidization with proximity to the fault.

Isotopic fractionation has been predicted to occur when FeS_2 forms from hydrocarbon derived H_2S (Goldhaber, Reynolds, and Rye, 1978). Fractionation controlled kinetically results in an enrichment in δS^{32} while fractionation controlled by isotopic equilibrium results in enrichment of δS^{34} of 5 to 15‰. A study by Price and Shieh (1979), in which they demonstrated the fractionation of sulfur isotopes during laboratory

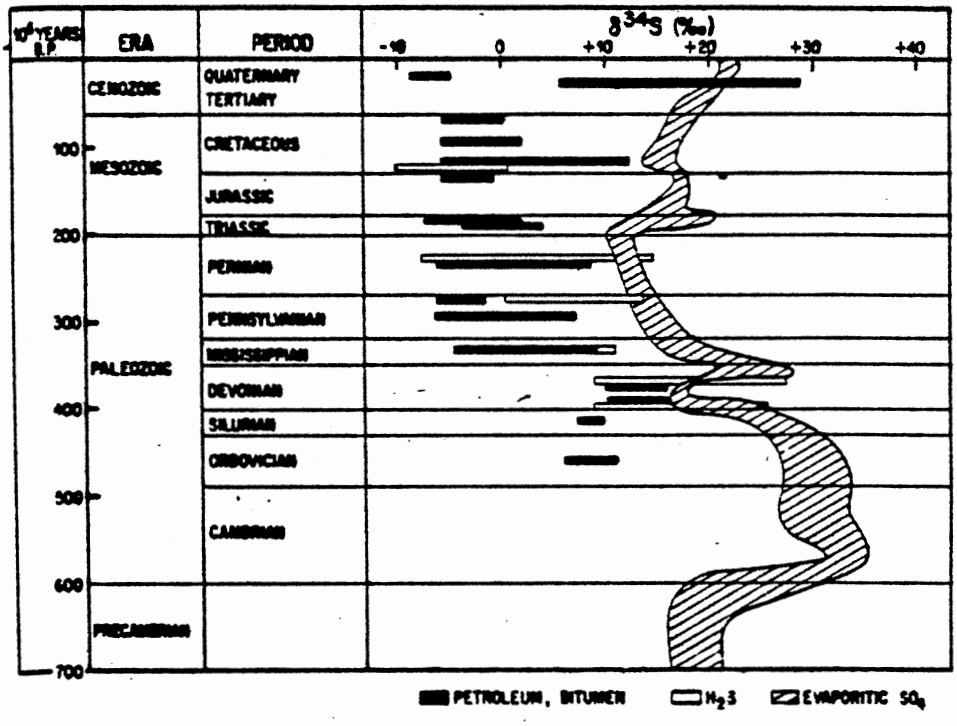

Fig. 23.--Comparison of sulfur isotopic abundances in reservoired petroleum and H_2S with evaporitic SO_4^{2-} by geological age (Krouse, 1977).

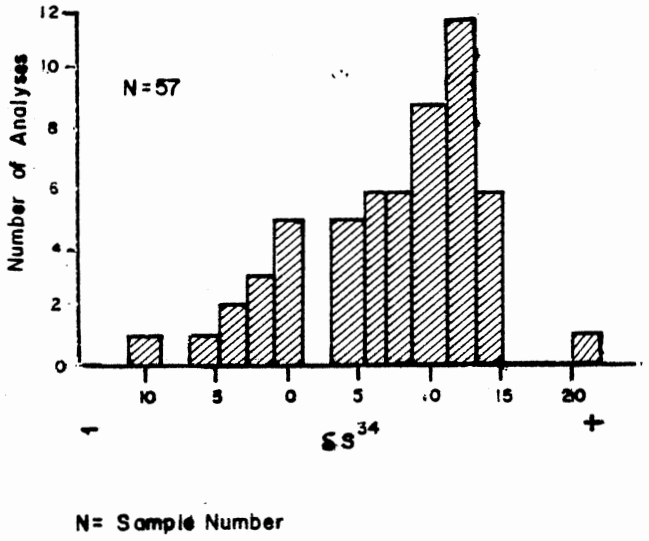

Fig. 24.--Frequency distribution for δS^{34} from H_2S gas associated with petroleum (after Goldhaber, Reynolds, and Rye, 1978).

synthesis of pyrite at low temperature, does not agree with the previous work. They studied the reaction of H_2S with geothite at 22^{o}-24^{o}C for periods from 0.5 hours to 65 days. Within two days fine-grained pyrite formed and was isotopically 0.8‰ lighter than the H_2S source. But after 65 days reaction time, the isotopic values for the H_2S and pyrite was nearly the same.

Results and Interpretation

Thirty-one pyrite samples, six oil samples, and two gypsum samples were analyzed for sulfur isotopes. The pyrite samples were collected from the surface and subsurface Permian formations investigated. Oil samples were collected from six producing wells from the Lower Permian (Noble Olson and Fortuna) and the Upper Pennsylvanian. Gypsum samples were collected from outcrops of the basal Cloud Chief Formation. Table IV lists the sulfur isotope data collected.

The frequency distribution of δS^{34} from pyrite samples is shown in Figure 25. The mean value is 2.5‰ and the standard deviation is $\pm$ 6.48.

Source of Sulfur in Oil

Thode and Monster (1965) compared the δS^{34} values of contemporaneous marine anhydrite and petroleum, ranging in age from Silurian to Permian and found the S^{32} in petroleum to be enriched by about 15‰. This enrichment was attributed to the action of sulfate reducing bacteria during the time of deposition of source rocks and subsequent formation of petroleum. The average δS^{34} of the crude oil and gypsum samples collected from Permian beds in the study area are 4.7‰ and 9.8‰,

TABLE IV

δS^{34} DISTRIBUTION IN PYRITE, CRUDE OIL, AND GYPSUM OF CEMENT AND CHICKASHA FIELDS

Sample Location	Formation Sampled	Sample Description	δS^{34}
	(Precision ± 0.2%)		
Williams B #1	Hennessey Shale	Pyrite	+2.4
	Garber Sandstone	Pyrite	+4.4
Thomas #1	Hennessey Shale	Pyrite	+3.9
	Garber Sandstone	Pyrite	+5.3
Smith #1	Hennessey Shale	Pyrite	-2.9
	Garber Sandstone	Pyrite	+3.9
Rider #1	Garber Sandstone	Pyrite	+4.3
Charleston #6	Hennessey Shale	Pyrite	+8.2
	Garber Sandstone	Pyrite	+7.3
Gray #2	Duncan Sandstone	Pyrite	-9.4
	Wellington Formation	Pyrite	+5.8
Kla-da-lug #3	Chickasha Formation	Pyrite	-0.4
Hemphill #1	Duncan Sandstone	Pyrite	-2.2
Melton #2	Hennessey Formation	Pyrite	+2.7
	Garber Sandstone	Pyrite	-1.8
	Wellington Formation	Pyrite	+3.0
Lemon #2	Duncan Sandstone	Pyrite	+8.8
	Hennessey Shale	Pyrite	+0.8
Henley #2	Chickasha Formation	Pyrite	+6.5
	Garber Sandstone	Pyrite	+8.3
	Wellington Formation	Pyrite	+6.3
Kunsmuller #1	Duncan Sandstone	Pyrite	-1.4
	Garber Sandstone	Pyrite	+9.7
W.J. Wood #1	Garber Sandstone	Pyrite	+8.5
Hartshorne #1	Duncan Sandstone	Pyrite	-3.4
	Garber Sandstone	Pyrite	+10.1
Pau Kune #12	Wellington Formation	Pyrite	+4.7
Kishketon #1	Wellington Formation	Pyrite	+8.7
	Wellington Formation	Pyrite by coal	-16.4
Surface SW,SW,NE	Rush Springs Formation	Pyrite nodule partially oxidized	-12.0
Surface NE,NE,NW 12-5N-9W	Rush Springs Formation	Pyrite	-9.3
Center 35N-9W	Noble Olson (Wellington Formation)	Crude oil	+3.1
Center 3-5N-9W	Fortuna (Wellington Formation)	Crude oil	+1.8
Surface SE,SE,SW 18-5N-9W	Cloud Chief Formation	Gypsum	+9.5
Surface NE,NE,NE	Cloud Chief Formation	Gypsum	+10.0

TABLE IV (continued)

Sample Location	Formation Sampled	Sample Description	δS^{34}
McKenna #1 5-5N-9W	Noble Olson (Wellington Formation)	Crude oil	+6.0
N. P. Royce #5 12-5N-9W	Noble Olson (Wellington Formation)	Crude oil	+3.2
South Rigney 12-5N-9W	Wade (Pennsylvanian)	Crude oil	+7.0
West Rigney #2 12-5N-9W, E,NW	Noble Olson (Wellington Formation)	Crude oil	+7.3

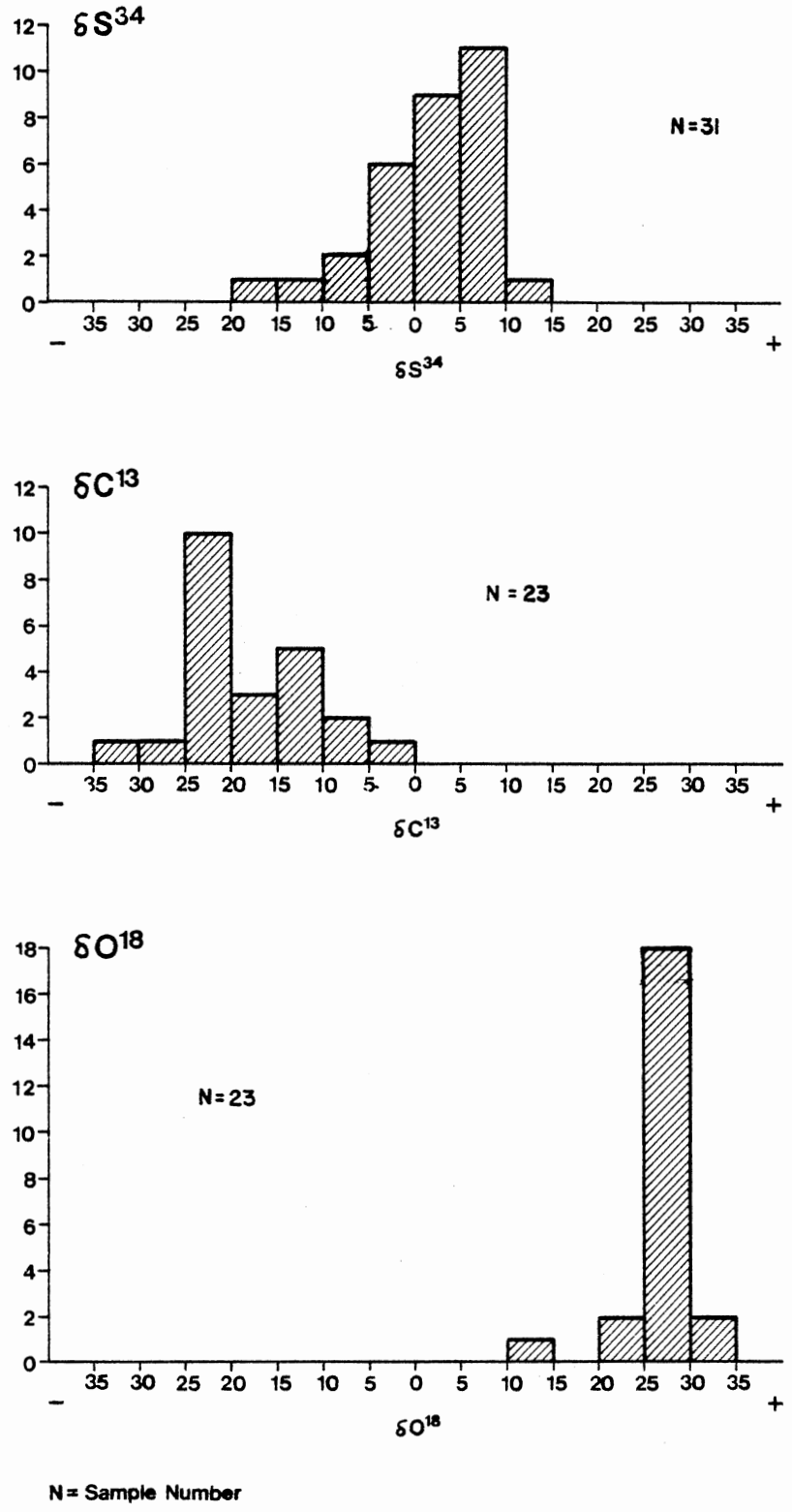

Fig. 25.--Frequency distributions of δO^{18}, δC^{13}, and δS^{34} from samples of carbonate and pyrite taken from Cement-Chickasha area.

respectively. Therefore, Permian shales could not have been the source of oil in the Lower Permian formations. The average crude oil value at Cement (δS^{34}) indicates a contemporaneous anhydrite or gypsum (from seawater sulfate) value of about 19‰ according to Thode and Monster (1965). Pennsylvanian shales appear to be the most likely source of oil since the average δS^{34} of worldwide Pennsylvanian seawater sulfate is 17‰ (Krouse, 1977, Fig. 23).

Source of Sulfur in Pyrite

The major source of sulfur in pyrite is the H_2S gas associated with the migrated hydrocarbons. Although no H_2S gas samples were collected from the study area, Thode and Monster (1970), and Krouse (1977) report that H_2S gas genetically related to petroleum has the same or only slightly heavier sulfur isotope content. Price and Shieh (1970) have shown that pyrite inorganically synthesized during the reaction of H_2S and goethite in aqueous media at approximately 25°C, has the same isotope composition as the H_2S. Therefore, comparing the average values of δS^{34} of sulfur in the pyrite (2.5 ‰) and of sulfur in the oil (4.7‰) strongly suggests that the H_2S associated with oil is the source of sulfur in pyrite. In addition, the frequency distribution histogram of sulfur in pyrite from the Cement-Chickaha Oil Field (Fig. 25) is remarkably similar to that of Goldhaber (1978) showing H_2S gas associated with petroleum reservoirs (Fig. 24).

One pyrite sample from the Wellington Formation occurs in association with coal. The δS^{34} of this sample is -16.4‰. The enrichment in S^{32} in this pyrite (and any similar pyrite which may be sampled) is the result of isotope fractionation by bacteria. Harrison and Thode (1958) proposed

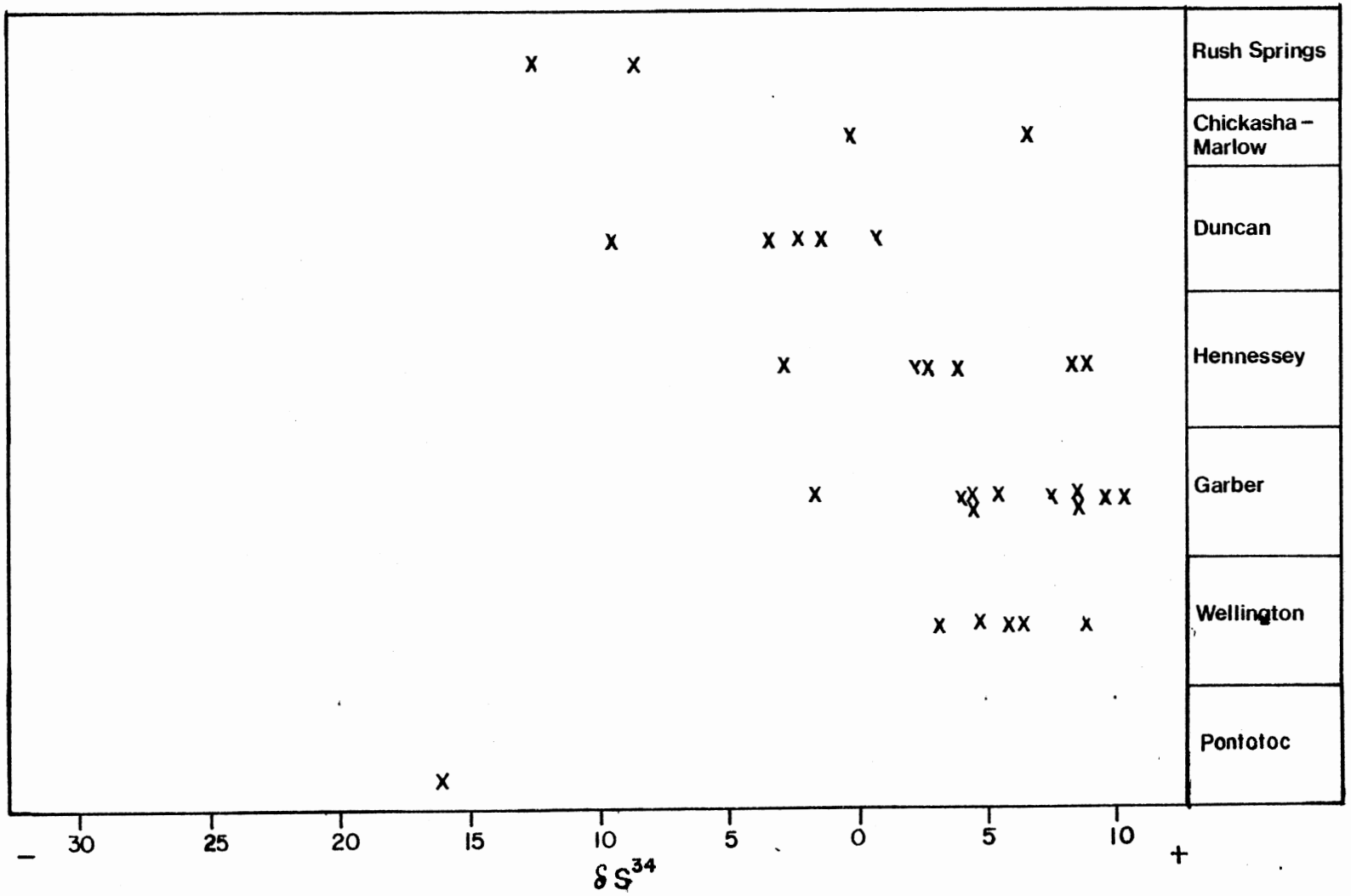

Fig. 26.--Stratigraphic distribution of δS^{34} in the study area for samples taken.

a fractionation model capable of explaining an enrichment of S^{32} up to 27‰. However, Kaplan and Rittenbura (1964) obtained S^{32} enrichment in H_2S of up to 46‰ relative to sulfate. It seems likely, therefore, that dissolved sulfate ions (SO_4^{--}) in water with isotopic ratios of δS^{34} = 9.5‰ will produce sulfide ions (S^{--}) with δS^{34} values varying between -17.5 to -37.5‰ by bacterial reduction.

Figure 26 shows the distribution of δS^{34} in the stratigraphic sections studied. It is evident that the δS^{34} values exhibit an enrichment in the lighter isotope with decreasing depth. The average value of the Duncan and Chickasha Formations is approximately 7‰ lighter than the average values of the Garber and Wellington Formations. This may be explained by: (1) an increase in biological activity with decreasing depth, or (2) an increase in the oxygen fugacity toward the shallow subsurface which would result in S^{32} enrichment (Ohmoto, 1972).

Carbon Isotopes

Theory

Carbon isotopic data has been used for many years in the study of petroleum. This technique has also been used on carbonate formations and cements as well as fossils.

Carbon values are expressed in terms of δ. This is defined by the C^{13}/C^{12} abundance ratio in the sample compared to the standard ratio in the Chicago PDB, (a Cretaceous belmenite from the Peedee Formation) with the values expressed in per mil (0/00). The equation used is the same as that given in the sulfur discussion.

The C^{13} that has been analyzed in previous studies has different sources. Coal, kerogen, oil, and natural gas have a carbon source, in

plants, which show a distinct preference for the C^{12} isotope during photosynthesis (Murata, 1969). Carbonates formed in a marine environment incorporate carbon from the CO_2 in the air or dissolved in water and show no isotopic preference. Fresh-water carbonates will contain carbon not only from the atmosphere but also from the CO_2 evolved during the decay of organic matter in soils.

The δC^{13} values of crude oils show a range of about -22 to -33‰ (Smith, 1978), while methane, which is isotopically lighter, has a δC^{13} less than -30‰ and as low as -90‰; natural gas has a range from -35 to -55‰, and is always lighter than oil because it is made predominantly of methane (Kirkland and Evans, 1976). Coals possess only a slightly greater δC^{13} value than crude oil (Smith, 1978). An extensive study by Keith and Weber (1964) showed an average δC^{13} value of $+0.6 \pm 2.8$‰ for marine carbonates, and an average value of -4.9 ± 2.8‰ for fresh-water carbonates. Carbonates that derive carbon from soil typically have δC^{13} values from -9 to 12‰ (Salomons, 1975).

Many studies have documented the occurrence of carbonate rocks and cements formed from the oxidation of hydrocarbons (Feely and Kulp, 1957; Hathaway and Degens, 1968); Manchur, 1969; Donovan, 1974; Donovan and Dalziel, 1977). When these reactions take place, carbon dioxide is evolved and reacts with water to produce bicarbonate. The bicarbonate bonds with magnesium and calcium in the ground waters and precipitates a carbonate cement that has an isotopic signature matching its parent hydrocarbon.

The alteration of gypsum to calcite has been studied (Feely and Kulp, 1957; Davis and Kirkland, 1970; Donovan, 1974; Kirkland and Evans, 1976). In these investigations the light δC^{13} values indicated the

calcite is a byproduct of the reduction of the calcium sulfate by natural gas or less likely oil.

Results and Interpretations

Crude oil and diagenetic carbonate samples were analyzed for carbon isotope ratios in order to determine the origin of the carbon in carbonates and their genetic relationship to a hydrocarbon source. The mean value of samples collected and those reported by Donovan (1972) is -19‰ (Table V). The frequency distribution of δC^{13} values of carbonates are shown in Figure 25. The mean value is -17.36‰ with a standard deviation of $\pm$ 7.02. Values range from -2 to -30‰. This wide range of δC^{13} values may reflect more than one carbon source or a mixture of sources.

In the previous chapter it was determined that the major carbonate cement mineral is calcite, but dolomite and ferroan dolomite are also observed in thin sections as cements. In addition, several zones of calcrete are identified in the Wellington Formation. One sample contains some marine fossil fragments. Examination of carbon isotopic ratios in the study area indicate a strong relationship between particular ranges of δC^{13} values and a specific type of carbonate mineralization. The majority of carbonate cements, both calcite and dolomite, in the Cement-Chickasha area, were strongly enriched in C^{12}. This isotopic composition resulted from effusive leakage of hydrocarbons through an unconformity and faults with subsequent oxidation and formation of carbonate cement (Donovan, 1978). Near the crest of the East Cement Dome the gypsum was replaced completely by calcium carbonate with complete preservation of the "crinkly bedding" of the initial gypsum. The reaction between hydro-

TABLE V

C^{13} AND O^{18} DISTRIBUTION IN CARBONATES AND CRUDE OIL OF CEMENT AND CHICKASHA FIELDS

Sample Location	Formation Sampled	Sample Description	C^{13}	O^{18}
Williams B #1	Garber Sandstone	Carbonate	-24.4	+29.9
Thomas #1	Garber Sandstone	Carbonate	-23.1	+26.5
Smith #1	Rush Springs Form.	Carbonate	-13.6	+26.2
	Garber Sandstone	Carbonate	-18.3	+29.1
Rider #1	Garber Sandstone	Carbonate	-21.6	+28.0
Charleston #6	Hennessey Shale	Carbonate	-22.0	+14.9
	Garber Sandstone	Carbonate	-20.8	+29.4
Gray #2	Duncan Sandstone	Carboante	-14.8	+28.7
Hemphill #1	Duncan Sandstone	Carbonate	-12.8	+26.5
Melton #2	Wellington Form.	Carbonate	- 1.8	+30.0
Lemon #2	Duncan Sandstone	Carbonate	-21.6	+30.6
Henley #2	Wellington Form.	Carbonate	-15.2	+29.6
Kunsmuller #1	Duncan Sandstone	Carbonate	-21.3	+26.0
W. J. Wood #1	Garber Sandstone	Carbonate	-18.4	+27.5
Hartshorne #1	Duncan Sandstone	Carbonate	-11.2	+25.5
	Garber Sandstone	Carbonate	-20.9	+27.0
Pau Kune #12	Wellington Form.	Carbonate	- 6.2	+28.5
Kishketon #1	Wellington Form.	Carbonate	-10.8	+28.0
	Wellington Form.	Carbonate	- 6.5	+28.1
Garret #1	Garber Sandstone	Carbonate	-22.3	+29.4
Surface SW,SW,NE 3-5N-9W	Cloud Chief Form.	Calcitized gypsum	-23.6	+24.4
Surface NE,NE,NW 12-5N-9W	Rush Springs Form.	Carbonate	-30.7	+24.3
Surface SW,NE,SW 35-6N-10W	Rush Springs Form.	Carbonate	-25.6	+26.4
Surface	Rush Springs Form.	Carbonate	-26.72	23.3
*Surface	Rush Springs Form.	Carbonate	-35.95	36.5
*Surface	Rush Springs Form.	Carbonate	-18.01	31.6
*Surface	Rush Springs Form.	Carbonate	-30.81	23.0
*Surface	Rush Springs Form.	Carbonate	- 8.43	26.8
*Surface	Rush Springs Form.	Carbonate	-30.14	33.6
*Surface	Rush Springs Form.	Carbonate	-11.33	25.4
*Surface	Rush Springs Form.	Carbonate	-13.21	25.7
*Surface	Rush Springs Form.	Carbonate	-39.22	32.8
*Surface	Rush Springs Form.	Carbonate	-29.41	28.9
*Surface	Rush Springs Form.	Carbonate	-21.41	28.3
*Surface	Rush Springs Form.	Carbonate	-34.54	30.5
*Surface	Rush Springs Form.	Carbonate	-15.66	26.1
*Surface	Rush Springs Form.	Carbonate	-16.60	25.3
*Surface	Rush Springs Form.	Carbonate	- 5.94	25.6
*Surface	Rush Springs Form.	Carbonate	-25.55	32.0
*Surface	Rush Springs Form.	Carbonate	-33.79	24.1

TABLE V (continued)

Sample Location	Formation Sampled	Sample Description	C^{13}	O^{18}
*Surface	Rush Springs Form.	Carbonate	-21.63	27.1
*Surface	Rush Springs Form.	Carbonate	-14.00	25.3
*Surface	Rush Springs Form.	Carbonate	- 5.47	25.1
*Surface	Rush Springs Form.	Carbonate	-15.88	25.3
*Surface	Rush Springs Form.	Carbonate	-30.07	24.5
*Surface	Rush Springs Form.	Carbonate	-24.52	32.8
*Surface	Rush Springs Form.	Carbonate	-21.27	27.2
*Surface	Cloud Chief Form.	Calcitized gypsum	-26.72	23.3
*Surface	Cloud Chief Form.	Calcitized gypsum	-35.47	25.8
*Rowe #1	Marlow Form.	Carbonate	-19.1	+29.2
NW,NW,NE	Chickasha Form.	Carbonate	-17.9	+32.1
36-6N-10W				
	Chickasha Form.	Carbonate	-17.8	+30.5
	Duncan Sandstone	Carbonate	-19.4	+20.8
	Garber Sandstone	Carbonate	-17.5	+31.1
	Wellington Form.	Carbonate	- 2.2	+29.3
*Amerada #1	Chickasha Form.	Carbonate	-14.1	+22.2
SW,SE,NE	Duncan Sandstone	Carbonate	-19.7	+30.3
1-Sn-9W	Wellington Form.	Carbonate	-11.7	+30.6
	Wellington Form.	Carbonate	- 9.1	+27.7
Center	Nobel-Olson	Crude oil	-30.2	--
3-5N-9W				
Center	Fortuna	Crude oil	-30.4	--
*Medrano #2	Fortuna	Crude oil	-29.4	--
*Pickard Edwards #2	Fortuna	Crude oil	-29.6	--
*Henley #6	Noble-Olson	Crude oil	-29.5	--
*Ginarch #5	Noble-Olson	Crude oil	-29.4	--
*Niles #1	Basal Permian Limestone	Crude oil	-29.7	
*Edwards #3	Griffin Sandstone+	Crude oil	-29.6	--
*McKenna #11	Fortuna	Crude oil	-29.4	--
*Pau Kune #1	Fortuna	Crude oil	-29.4	--
*McKenna #18	Marchand+	Crude oil	-30.3	--
*Pau Kune #11	Marchand+	Crude oil	-30.3	--
*L. Miller #1	Marchand+	Crude oil	-29.5	--
*Hare #1	Marchand+	Crude oil	-29.5	--

*Denotes data taken from Donovan, 1974.

+Denotes Pennsylvanian Formations (all others are Permian). Fortuna and Noble-Olson are inside the Wellington Formation. See Table I for well locations.

carbon and sulfate to form calcite, water, and hydrogen sulfide (Annels, 1974) is:

$$CH_4 + CaSO_4 \rightarrow CaCO_3 + H_2S + H_2O \qquad G = -6.0 \text{ Kcal/mole} \qquad (12)$$

Calcrete samples from the Wellington Formation show a δC^{13} value between -4 and -10‰ which suggests a fresh water carbonate origin (Keith and Weber, 1964). One sample showing fossil fragments yields a δC^{13} value of -1.8‰ implying a marine origin. A group of values cluster between -10 to -15‰ suggesting a bimodal carbon source from both hydrocarbon and fresh water.

The following model is proposed to explain the genesis for the isotopic composition of hydrocarbon derived, fresh water, and hybrid type carbonates. The average value for fresh water carbonates is -4.9‰ $\pm$ 2.8 as reported by Keith and Weber (1964). The carbonate enriched in C^{12} from hydrocarbon oxidation, as reported by this study and Donovan (1978), has a δC^{13} value of -32‰. Therefore, the δC^{13} of each sample analyzed may be evaluated in terms of two end members as shown by the following equation (Al-Shaieb, 1981):

$$-32 * X + -4.9 * (1-X) = Z$$

where X represents the fraction of hydrocarbon contribution and Z the measured δC^{13}. The graphic representation of this equation is shown in Fig. 27). The isotopic data plotted on Figure 27 appear to cluster in three regions: region A represents hydrocarbon derived carbon, region B fresh water derived carbon, and region C represents a hybrid source of carbon. This hybrid source combines carbon made available from the oxidation of hydrocarbon and the dissolution of earlier calcrete deposits (see Equation 3).

The distribution of δC^{13} in the stratigraphic section investigated

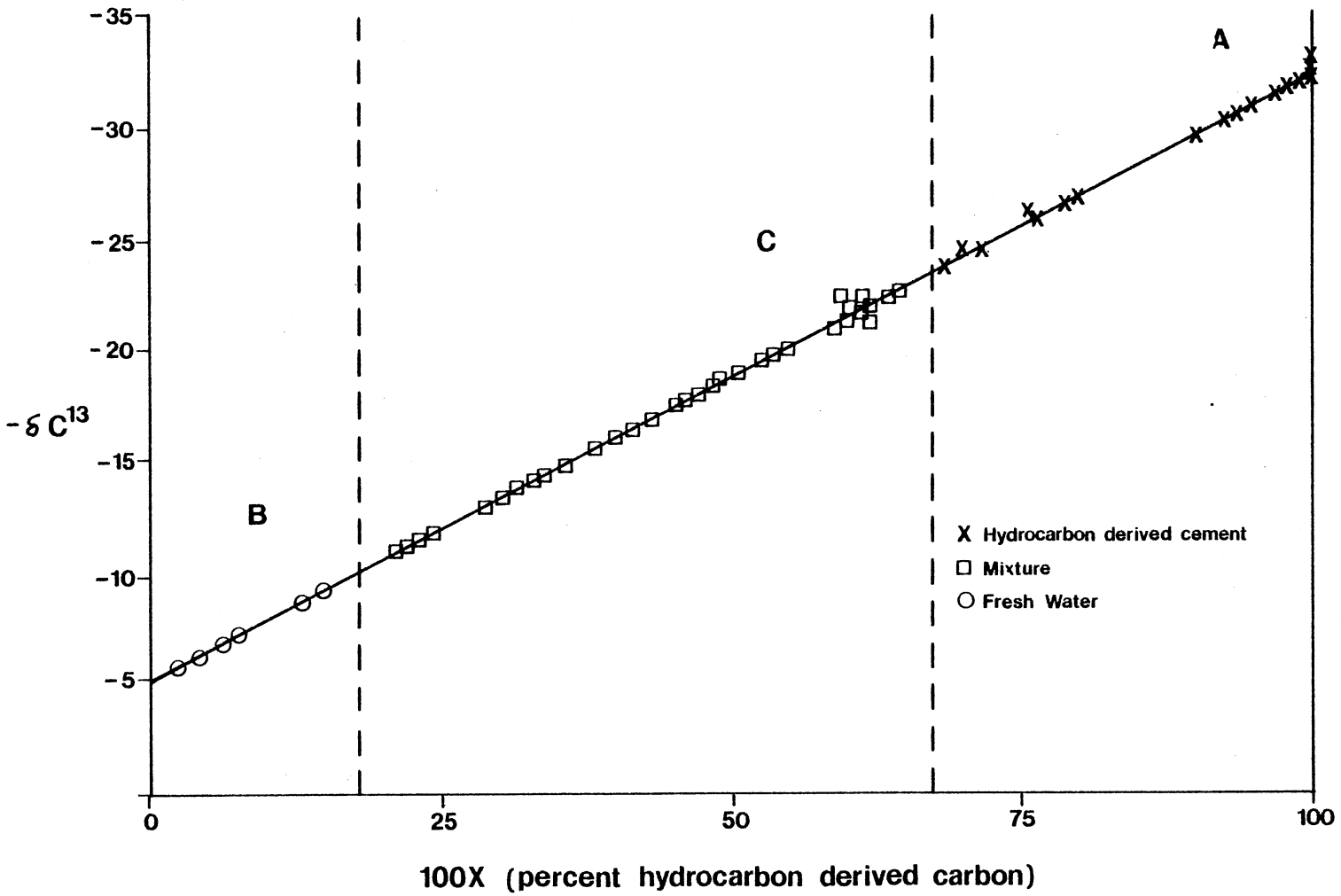

Fig. 27.--Percent hydrocarbon derived carbon in carbonate samples in terms of two end members (-32 and -4.9) according to the equation -32 * X + -4.9 * (1-X) = Z where X represents the hydrocarbon contribution and Z the measured δC^{13} (Al-Shaieb, 1981).

is shown in Figure 28. It is very evident that the carbonates in the Wellington Formation are fresh water derived while the other formations show the influence of a hydrocarbon source and the results of the hybridization.

Oxygen Isotopes

Theory

The δO^{18} values represent a relative comparison of the O^{18}/O^{16} ratio to the standard ratio of SMOW (standard mean ocean water). These values are given in per mil (0/00).

The oxygen isotopes of calcite are acquired from its depositional waters. Therefore, these oxygen isotopes can indicate whether water had a fixed isotopic composition and temperature or if there was more than one episode of calcite precipitation from different waters. The final carbonate isotopic composition is largely dependent on three factors: (1) temperature of the depositional water, (2) mixing of waters, (3) hydrocarbon induced evaporation of formation waters (Donovan and Dalzier, 1977; Goldhaber, Reynolds, Rye, and Grauch, 1979).

Seawater has a constant isotopic composition of 0 $\pm$ 1‰ relative to SMOW (Epstein and Mayeda, 1953). Because H_2O^{16} has a higher vapor pressure than H_2O^{18}, meteoric waters are somewhat lighter than seawater. There is also a latitude dependent change governed by temperature. The δO^{18} in the carbonates precipitated from these waters reflect their origin.

Murata and others (1969) show that δO^{18} values of fresh water and diagenetic carbonate may vary from +9 to +36‰. Goldhaber and others (1979) indicated that δO^{18} values of calcite in a south Texas roll-type uranium deposit (Benevides) reflect precipitation from meteoric ground

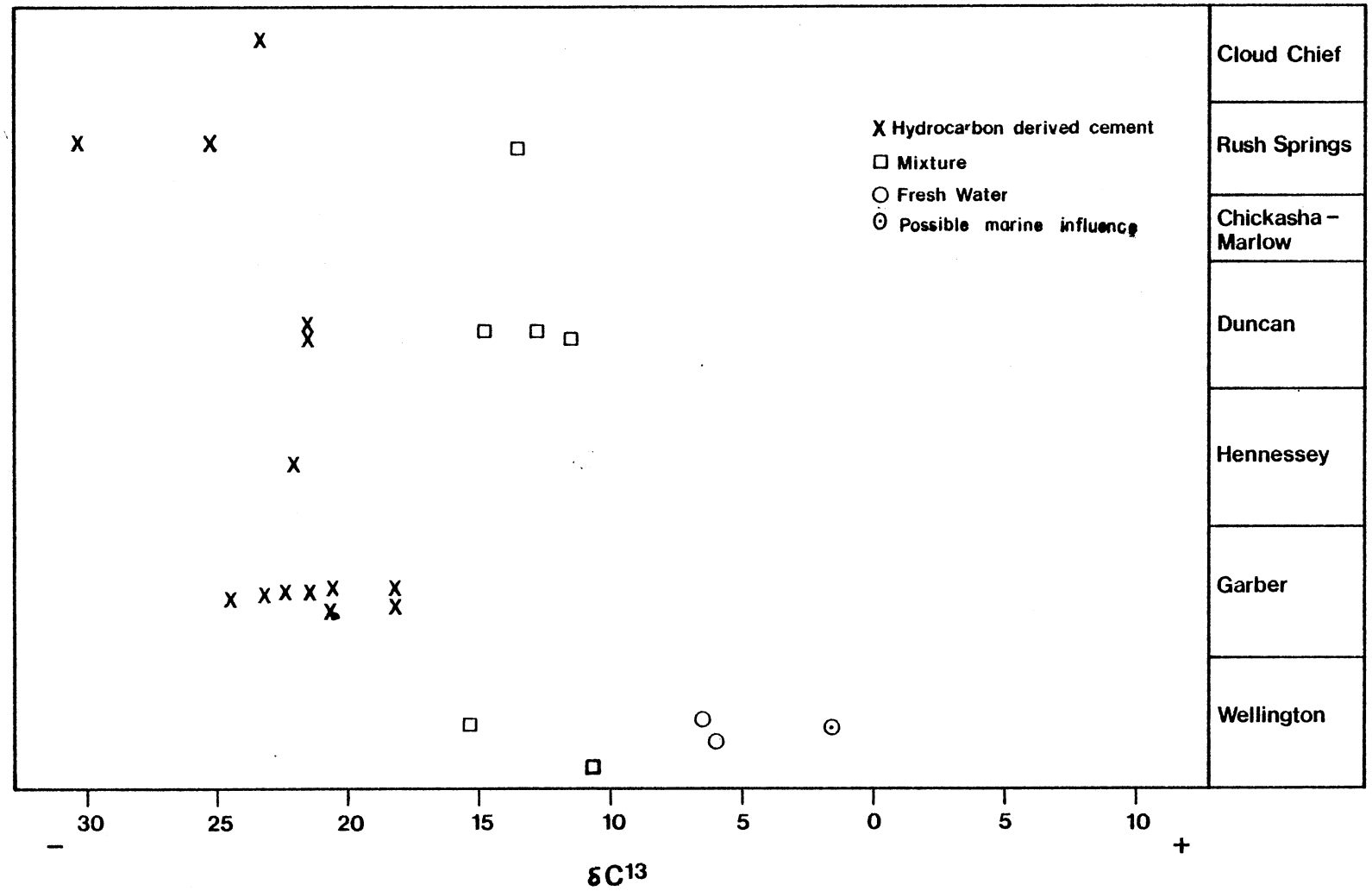

Fig. 28.--Stratigraphic distribution of δC^{13} for samples taken in the study area.

waters. These values show a narrow range from -24.4 to -25.1‰.

The δO^{18} composition of a subsurface carbonate forming solution can be changed by mixing with other brines or with meteoric waters (Donovan and Dalziel, 1977). Formation waters often show an enrichment in O^{18} (Clayton et al., 1966). This enrichment is believed to have resulted from partial evaporation of pore water and isotopic equilibrium with minerals in the surrounding sediments.

A process proposed by Mills and Wells (1919) and later supported by Nisle (1941) and Donovan (1972) involves gas-induced evaporation of ground water to provide an increase in O^{18} in formational waters. In this process, natural gas from depth expands and separates from solution as it rises through ground water. This causes selective evaporation of H_2O^{16} over H_2O^{18} due to their differing vapor pressures (Rayleigh distillation).

Results and Interpretations

All carbonate samples collected were analyzed for their oxygen isotopic composition. Figure 25 shows the frequency distribution of δO^{18} values while the stratigraphic distribution of these values is shown in Fig. 29. The mean value of the δO^{18} of the samples is 29.1‰ with a standard deviation of $\pm$ 3.34. Because oxygen isotopes of calcite are inherited from depositional waters, the narrow range and constancy of the δO^{18} (Table V) indicate very clearly that calcite was deposited from water of a fixed isotopic composition and temperature. The isotopic composition of formation water in equilibrium with precipitated calcium carbonate may be estimated using the mean annual temperature reported by Donovan (1972) and an isotopic separation curve for oxygen isotopes in

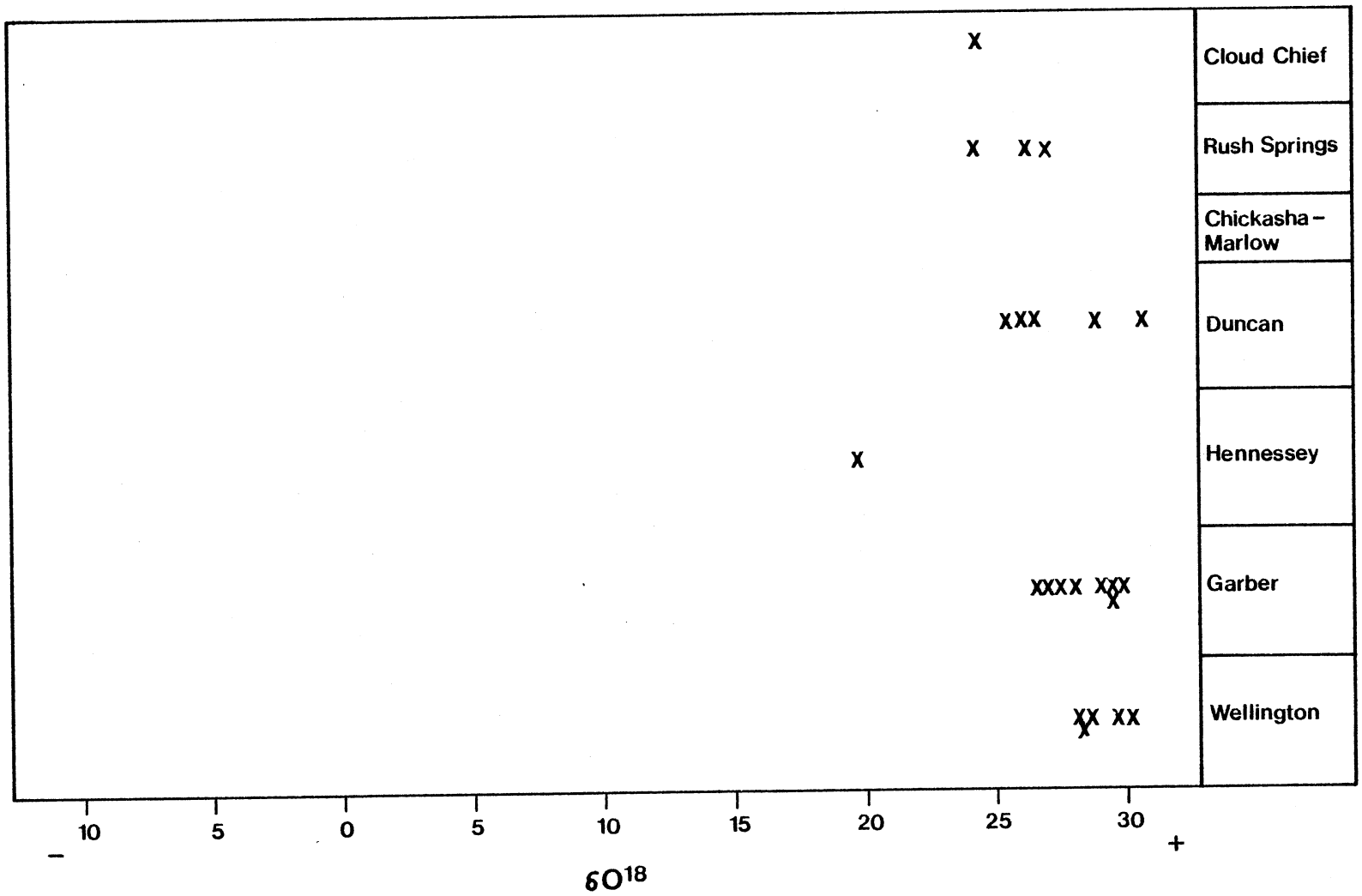

Fig. 29.--Stratigraphic distribution of δO^{18} for samples taken in the study area.

calcite and water ($\Delta = \delta O^{18}$ calcite $= \delta O^{18}$ water) as a function of temperature (Goldhaber et al., 1979; Fig. 30). The calculated O^{18} of the formation water using $T^{o}C = 16.4$ and δO^{18} calcite = 27.1‰ is approximately -3.4‰. Donovan (1974) suggested that Cement carbonates have normal O^{18}/O^{16} ratios. On the other hand, he indicated that gas released from liquid hydrocarbons by depressurization may induce ground water evaporation which results in higher δO^{18} values.

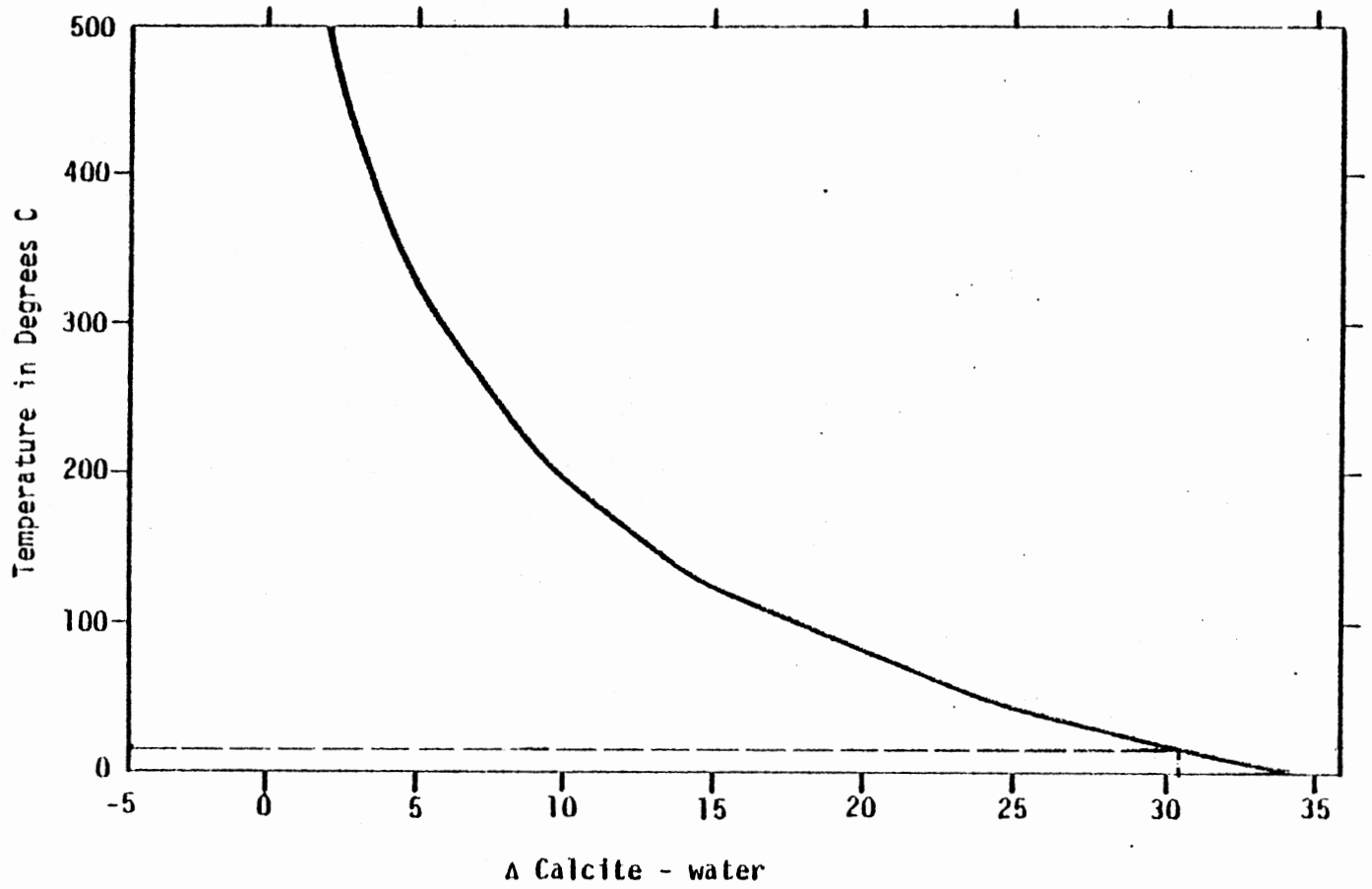

Fig. 30.--Isotopic separation of oxygen isotopes in calcite and water, ($\Delta = \delta^{18}O$ calcite $- \delta^{18}O$ water) as a function of temperature, with the mean annual temperature at Cement shown (after Goldhaber, Reynolds, Rye, and Grauch, 1979).

CHAPTER VI

CONCLUSIONS

The Cement-Chickasha Oil Fields offer a good example of diagenetic alteration of shallow Permian beds as direct evidence of hydrocarbon migration primarily along an unconformity and fault zones. The three primary alteration types observed are: (1) introduction of large amounts of diagenetic carbonates as a cement and/or as a replacement of detrital minerals; (2) the discoloration of Permian red beds; (3) the formation of pyrite as cement and/or as disseminated cubes.

The oxidation of hydrocarbons to carbon dioxide is the main source of carbon in diagenetic carbonates. These occur as cement and as replacements of gypsum by calcite. They also show an enrichment in C^{12}. Some of these δC^{13} values also suggest influence from fresh water or marine carbonates in the Wellington Formation. Isotopically hybrid carbonate cement with a bimodal carbon source is also found throughout the section. Hydrocarbon and fresh water are proposed as the sources of carbon of this type. The δO^{18} values indicate the carbonates were precipitated from formational waters of a fixed isotopic composition.

Hydrogen sulfide gas associated with petroleum was the impetus for two related alteration events. This gas served as a reducing agent. The bleaching of the Permian beds and the formation of pyrite both occur as a result of the reduction of iron oxide by hydrogen sulfide. The sulfur isotopes from petroleum at depth and the diagenetic pyrite show a close

relationship. The δS^{34} values of pyrite collected from the surface and shallow subsurface tend to be slightly enriched in S^{32}, due to either increases in biological activity or oxygen fugacity.

Authigenic kaolinite and mixed-layer illite-smectite are the byproduct of hydrocarbon migration which had drastic effect on the geochemistry of formation water. Nearly all detrital illite, characteristic of the red bed environment, was altered or replaced by diagenetic products.

Finally, these diagenetic minerals related to hydrocarbon migration may be used as a path finder for hydrocarbon accumulations in other sites with a similar geological setting.

BIBLIOGRAPHY

Allen, R. F., 1980, Uranium potential of the Cement District, southwestern Oklahoma: Unpublished M.S. thesis, Oklahoma State University, 84 p.

Al-Shaieb, Z., 1981, Personal communication.

Al-Shaieb, Z., et al., 1977, Uranium potential of Permian and Pennsylvanian sandstones in Oklahoma: Am. Assoc. Petroleum Geologists Bull., v. 61, p. 360-375.

Al-Shaieb, Z., et al., 1978, Guidebook to uranium mineralization in sedimentary and igneous rocks of Wichita Mountains region, southwestern Oklahoma: Published by Oklahoma City Geological Society, p. 61-73.

Al-Shaieb, Z., R. E. Hanson, R. N. Donovan, J. W. Shelton, 1980, Petrology and diagenesis of sandstones in the Post Oak Formation (Permian), southwestern Oklahoma: Jour. Sed. Petrology, v. 50, p. 43-50.

Al-Shaieb, Z., J. W. Shelton, et al., 1977, Evaluation of uranium potential in selected Pennsylvanian and Permian units and igneous rocks in southwestern and southern Oklahoma: Bendix Field Engineering Corporation, Subcontract #76-024-E, Open-File Report, 248 p.

Baker, E. G., 1969, A geochemical evaluation of petroleum migration and accumulation, in B. N Nagy and U. Colombo, eds., Fundamental aspects of petroleum geochemistry: New York, Elsevier, p. 299-329.

Boles, J. R., and S. G. Franks, 1979, Clay diagenesis in Wilcox Sandstones of southwest Texas: Implications of smectite diagenesis on sandstone cementation: Jour. Sed. Petrology, v. 49, p. 55-70.

Bredehoeft, J. D., C. R. Blyth, W. A. White, and G. B. Maxey, 1963, Possible mechanism for concentration of brines in subsurface formations: Am. Assoc. Petroleum Geologists Bull., v. 47, p. 257-269.

Bunn, J. R., 1930, Jefferson County, in Oil and Gas in Oklahoma: Oklahoma Geol. Survey Bull. 40, p. 341-381.

Burst, J. F., 1969, Diagenesis of Gulf Coast clayey sediments and its possible relation to petroleum migration: Am. Assoc. Petroleum Geologists Bull., v. 53, p. 73-93.

Chase, G. W., 1954, Permian conglomerates around Wichita Mountains, Oklahoma: Am. Assoc. Petroleum Geologists Bull., v. 38, p. 2028-2035.

Cheney, E. S., and M. L. Jensen, 1966, Stable isotopic geology of the gas hills, Wyoming, uranium district: Econ. Geol., v. 61, p. 44-71.

Clayton, R. N., and I. Friedman, et al., 1966, The origin of saline formation waters-I, Isotopic composition: Jour. Geophys. Research, v. 71, p. 3869-3882.

Davis, J. B., and D. W. Kirkland, 1970, Native sulfur deposition in Castille Formation, Culberson County, Texas: Economic Geol., v. 65, p. 107-121.

Davis, L. V., 1955, Geology and groundwater resources of Grady and northern Stephens Counties, Oklahoma: Oklahoma Geol. Survey. Bull. 73, p. 184.

Davis, L. V., and H. H. Tanaka, 1963, Ground water resources of the Rush Springs sandstone in the Caddo County area, Oklahoma: Oklahoma Geol. Survey Bull. 61, 63 p.

DeSitter, L. U., 1947, Diagenesis of oil-field brines: Am. Assoc. Petroleum Geologists, v. 31, p. 2030-2040.

Donovan, T. J., 1972, Surface mineralogical and chemical evidence for buried hydrocarbons, Cement Field Oklahoma: Ph.D. thesis, University of California, Los Angeles,p. 117.

Donovan, T. J., 1974, Petroleum microseepage at Cement, Oklahoma: Evidence and mechanism: Am. Assoc. Petroleum Geologists Bull., v. 58, p. 429-446.

Donovan, T. J., et al., 1979, Aeromagnetic detection of diagenetic magnetic over oil fields: Am. Assoc. Petroleum Geologists Bull., v. 63, p. 245-248.

Donovan, T. J., and M. C. Balziel, 1977, Late diagenetic indicators of buried oil and gas: U.S. Geol. Survey Open-File Report 77-817, 44 p.

Dott, R. H., 1930, Garvin County, in Oil and Gas in Oklahoma: Oklahoma Geol. Survey Bull. 40, p. 119-143.

Epstein, S., and T. Mayeda, 1953, Variation of O^{18} content of waters from natural sources: Geochim et Cosmichim. Acta, v. 4, p. 225-240.

Fay, R. O., 1964, The Blaine and related formations of northwestern Oklahoma and southern Kansas: Oklahoma Geol. Survey Bull. 98, 238 p.

Fay, R. O., 1968, The Geology of region II, in Appraisal of water and related land resources in Oklahoma: Oklahoma Water Resources Board Publ. 24, p. 21-24.

Freely, H. W. and J. L. Kulp, 1957, Origin of Gulf Coast salt-dome deposits: Am. Assoc. Petroleum Geologists Bull., v. 41, p. 1802-1853.

Ferguson, J. D., 1977, The subsurface alteration and mineralization of Permian red beds overlying several oil fields in southern Oklahoma: Unpublished M.S. thesis, Oklahoma State University, 95 p.

Flood, J. R., 1969, Areal geology of western Jerrerson County, Oklahoma: Unpublished M.S. thesis, University of Oklahoma, 61 p.

Fuex, A. N., 1977, The use of stable carbon isotopes in hydrocarbon exploration: Jour. Geochem. Exploration, v.7, p. 155-188.

Goldhaber, M. B., R. L. Reynolds, and R. O. Rye, 1978, Origin of a South Texas roll-type uranium deposit: II. Sulfide petrology and sulfur isotopes studies: Econ. Geol., v. 73, p. 1690-1705.

Goldhaber, M. B., R. L. Reynolds, R. O. Rye, and R. I. Grauch, 1979, Petrology and isotope geochemistry of calcite in a South Texas roll-type uranium deposit: U.S. Geol. Survey Open-File Report 79-828, 21 p.

Gould, C. N., 1924, A new classification of the Permian red beds of southwestern Oklahoma: Am. Assoc. Petroleum Geologists Bull., v. 8, p. 322-341.

Ham, W. E., 1960, Middle Permian evaporites in southwestern Oklahoma, in Report of the Twenty-First session Norden: Part 12, International Geologic Congress, Copenhagen, p. 138-151.

Hanson, R. E., Z. Al-Shaieb, 1980, Voluminous subalkaline silicic magmas related to intracontinental rifting in the southern Oklahoma aulacogen: Geology, v. 8, p. 180-184.

Harlton, B. H., 1960, Stratigraphy of Cement pool and adjacent area, Caddo and Grady Counties, Oklahoma: Am. Assoc. Petroleum Geologists Bull., v. 44, p. 210-226.

Harrison, A. G., and H. G. Thode, 1958, Sulfur isotope abundances in hydrocarbons and source rocks of Uinita Basin, Utah: Am. Assoc. Petroleum Geologists Bull., v. 42, p. 2642-2649.

Herrmann, L. A., 1961, Structural geology of Cement-Chickasha area, Caddo and Grady Counties, Oklahoma: Am. Assoc. Petroleum Geologists Bull., v. 45, p. 1971-1993.

Hinch, H. H., 1980, The nature of shales and the dynamics of hydrocarbon expulsion in the Gulf Coast Tertiary Section: Problems of Petroleum Migration, p. 1-18.

Hower, J., et al., 1976, Mechanisms of burial, Part I mineralogical and chemical evidence: Bull. Geol. Soc. Amer., v. 87, p. 725-737.

Irwin, H., C. Curtis, and M. Caleman, 1977, Isotopic evidence for source of diagenetic carbonates formed during burial of organic-rich sediments: Nature, v. 269, p. 209-213.

Kaplan, I. R., and S. C. Rittenberg, 1963, Basin sedimentation and diagenesis in The sea; ideas and observations on progress in the study of the seas (M. N. Hill, ed.), v. 3, p. 583-619.

Keith, M. L., and J. N. Weber, 1964, Carbon and oxygen isotopic composition of selected limestones and fossils: Geochim et Cosmochim. Acta, v. 28, p. 1787-1816.

Kirkland, D. W., and R. Evans, 1976, Origin of limestone buttes, Gypsum plain, Culberson County, Texas: Am. Assoc. Petroleum Geologists Bull., v. 60, p. 2005-2018.

Kittrick, J. A., and E. W. Hope, 1963, A procedure for the particle-size separation of soils for X-ray diffraction analysis: Clay Min. Bull. v. 10, p. 319-325.

Krouse, H. R., 1977, Sulfur isotope studies and their role in petroleum exploration: Jour. Geochem. Exploration, v. 7, p. 189-211.

MacLachlan, M. E., 1967, Oklahoma, in Paleotectonic investigations of the Permian system in the United States: U.S. Geol. Survey Prof. Paper 515-E, p. 85-92.

Magara, K., 1980, Agent for primary hydrocarbon migration: a review: Problems of Petroleum Migration, AAPG Studies in Geology, No. 10, p. 32.

Manchur, G. P., 1969, Isotopic composition of carbon in calcite paragenetic with sulfur: Geochemistry Internat., v. 6, p. 660-670.

Mills, R. V. A., and R. C. Wells, 1919, The evaporation and concentration of waters associated with petroleum and natural gas: U.S. Geol. Survey Bull. 693, 104 p.

Miser, H. D., 1954, Geologic map of Oklahoma: U.S. Geol. Survey and Oklahoma Geol. Survey.

Munn, M. J., 1914, Reconnaissance of the Grandfield District, Oklahoma: U.S. Geol. Survey Bull. 547, 85 p.

Murata, K. J., I. Friedman, and B. M. Madsen, 1969, Isotopic composition of diagenetic carbonates in marine Miocene Formations of California and Oregon: U.S. Geol. Survey Prog. Paper 614-B, 24 p.

Nisle, R. G., 1941, Considerations on the vertical migration of gases: Geophysics, v. 6, p. 449-454.

O'Brien, B. E., 1963, Geology of east-central Caddo County, Oklahoma: Unpublished M.S. thesis, University of Oklahoma, 72 p.

Ohomoto, H., 1972, Systemacs of sulfur and carbon isotopes in hydrothermal ore deposits: Econ. Geol., v. 67, p. 551-578.

Olmstead, R. W., 1975, Geochemical studies of uranium in south-central Oklahoma: Unpublished M.s. thesis, Oklahoma State University, 116 p.

Orr, W. L., 1974, Changes in sulfur content and isotopic ratios during petroleum migration--study of Big Horn Basin Paleozoic oils: Am. Assoc. Petroleum Geologists Bull., v. 50, p. 2295-2318.

Perry, E., and J. Hower, 1970, Burial diagenesis in Gulf Coast pelitic sediments: Clays and clay minerals, v. 18, p. 165-177.

Powell, B. N., and D. W. Phelps, 1977, Igneous cumulates of Wichita Province and their tectonic implications: Geology, v. 5, p. 52-56.

Price, F. T. and Y. N. Shieh, 1979, Fractionation of sulfur isotopes during laboratory synthesis of pyrite at low temperatures: Chemical Geology, v. 27, p. 245-253.

Reeves, F., 1922, Geology of the Cement oil field, Caddo County, Oklahoma: U.S. Geol. Survey Bull. 726, pt. 2, p. 41-85.

Reynolds, T. L., and M. B. Goldhaber, 1978, Origin of a South Texas roll-type uranium deposit: I. Alteration of iron-titanium oxide minerals: Econ. Geol., v. 73, p. 1677-1689.

Salomons, W., 1975, Chemical and isotopic composition of carbonates in recent sediments and soils from Western Europe: Jour. Sed. Petrology,v. 45, p. 440-449.

Self, R. P., 1966, Petrology of the Duncan Sandstone (Permian) of South-Central Oklahoma: Unpublished M.S. thesis, University of Oklahoma, 133 p.

Shvartsev, S. L., and V. A. Bazhenov, 1978, Geochemical conditions for the formation of illite in weathering-crust products, Geochem. Inter., v. 15, p. 49-56.

Smith, J. W., 1978, Carbonates--a guide to hydrocarbons: Jour. Geochem. Exploration, v. 14, p.103-107.

Thode, H. G., and J. Monster, 1970, Sulfur isotope abundances and genetic relations of oil accumulations in Middle East basin: Am. Assoc. Petroleum Geologists Bull., v. 54, p. 627-637.

Thode, H. G., and J. Monster, 1965, Sulfur-isotope geochemistry of petroleum, evaporites and ancient seas, in A. Young and J. E. Galley, eds., Fluids in subsurface environments: Am. Assoc. Petroleum Geologists Mem. 4, p. 367-377.

Thode, H. G., J. Monster, and H. B. Dunford, 1958, Sulfur isotope abundances in petroleum and associated materials: Am. Assoc. Petroleum Geologists Bull., v. 42, p. 2619-2641.

Thomas, R. G., 1981, Personal communication.

Vrendenburgh, L. D., and E. S. Cheney, 1971, Sulfur and carbon isotopic investigation of petroleum, Wind River basin, Wyoming: Am. Assoc. Petroleum Geologists Bull., v. 55, p. 1954-1975.

Wickham, J., M. Pruatt, R. Leon, and T. Thompson, 1975, The southern Oklahoma aulacogen: Absts. with Programs: An. Mtg. Geol. Soc. America, v. 7, p. 1332.

VITA

Ralph Anthony Lilburn

Candidate for the Degree of

Master of Science

Thesis: MINERALOGICAL, GEOCHEMICAL, AND ISOTOPIC EVIDENCE OF DIAGENETIC ALTERATION ATTRIBUTABLE TO HYDROCARBON MIGRATION, CEMENT-CHICKASHA FIELD, OKLAHOMA

Major Field: Geology

Biographical:

Personal Data: Born in Nowata, Oklahoma, December 29, 1955, the son of Mr. and Mrs. Ralph L. Lilburn.

Education: Graduated from Nowata High School, Nowata, Oklahoma, in May, 1974; received Bachelor of Science degree in Geology from Oklahoma State University in July, 1979; completed the requirements for the Master of Science degree in Geology at Oklahoma State University in May, 1981.

Professional Experience: Geological technician, Jay Robertson Consulting, Nowata, Oklahoma, May, 1978 to August, 1978; Contract Field Geologist, Mapco, Ketchikan, Alaska, July, 1979 to August, 1979; Teaching Assistant, Department of Geology, Oklahoma State University, Stillwater, Oklahoma, August, 1979 to May, 1980; Research Assistant, Department of Geology, Oklahoma State University, Stillwater, Oklahoma, April, 1980 to April, 1981; junior member of the American Association of Petroleum Geologists.

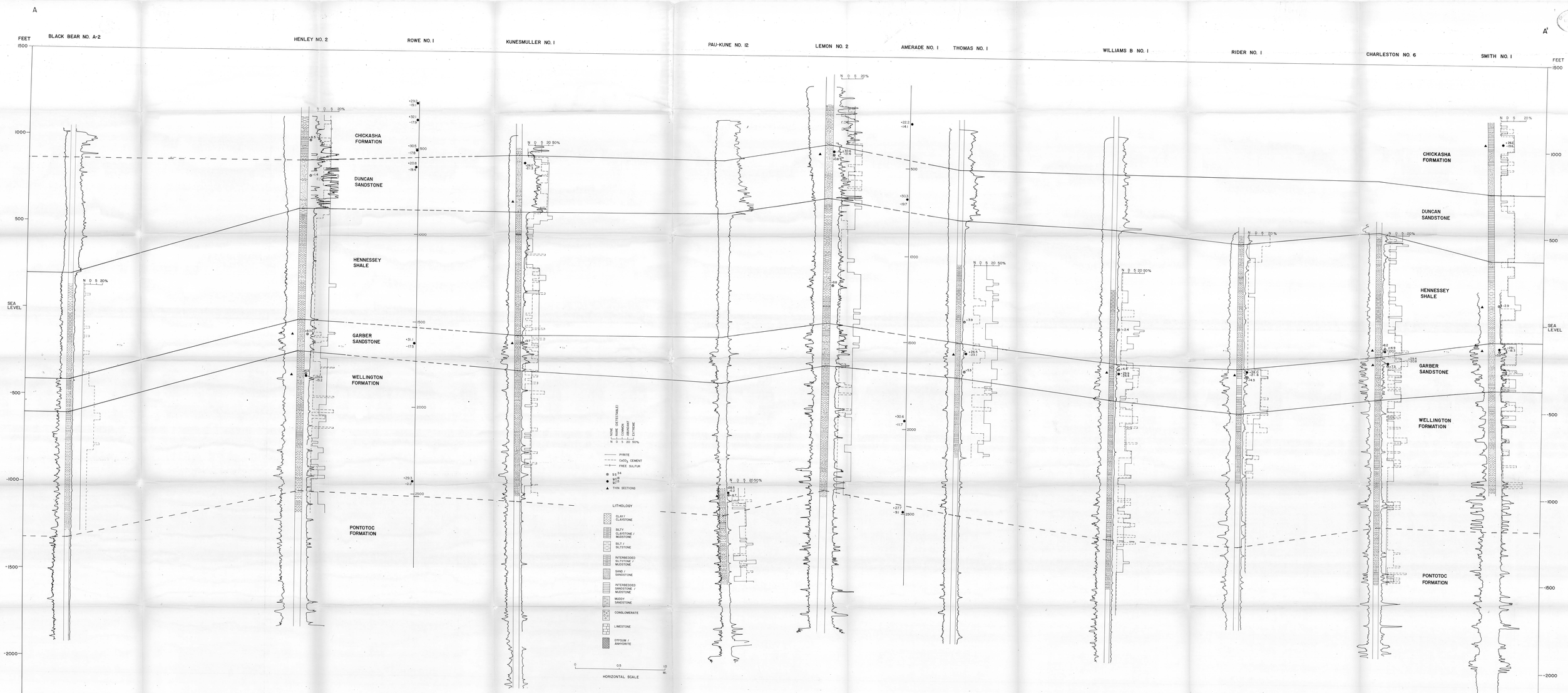

PLATE I. WEST-EAST CROSS-SECTION (A-A') OF THE PERMIAN SECTION AT THE CEMENT-CHICKASHA ANTICLINES

CYRIL QUADRANGLE

LAVERTY QUADRANGLE

R.10 W. R.9 W. R.9 W. R.8 W.

T.6 N.

T.5 N.

T.5 N.

T.4 N.

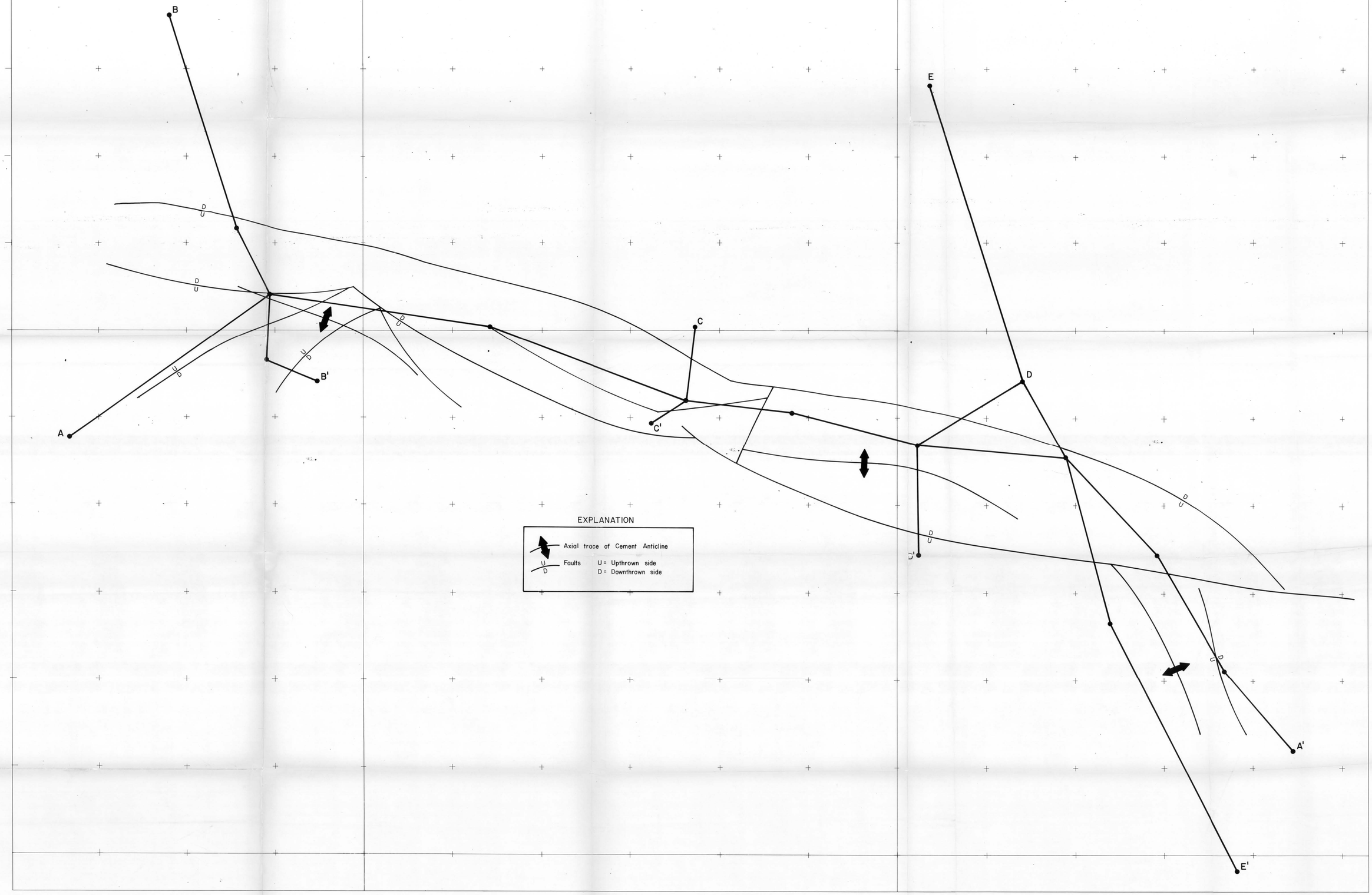

Plate 4. MAP OF PRE-PERMIAN STRUCTURE, LOCATION OF CROSS-SECTIONS AND ALL WELLS STUDIED, CEMENT-CHICKASHA OIL FIELDS

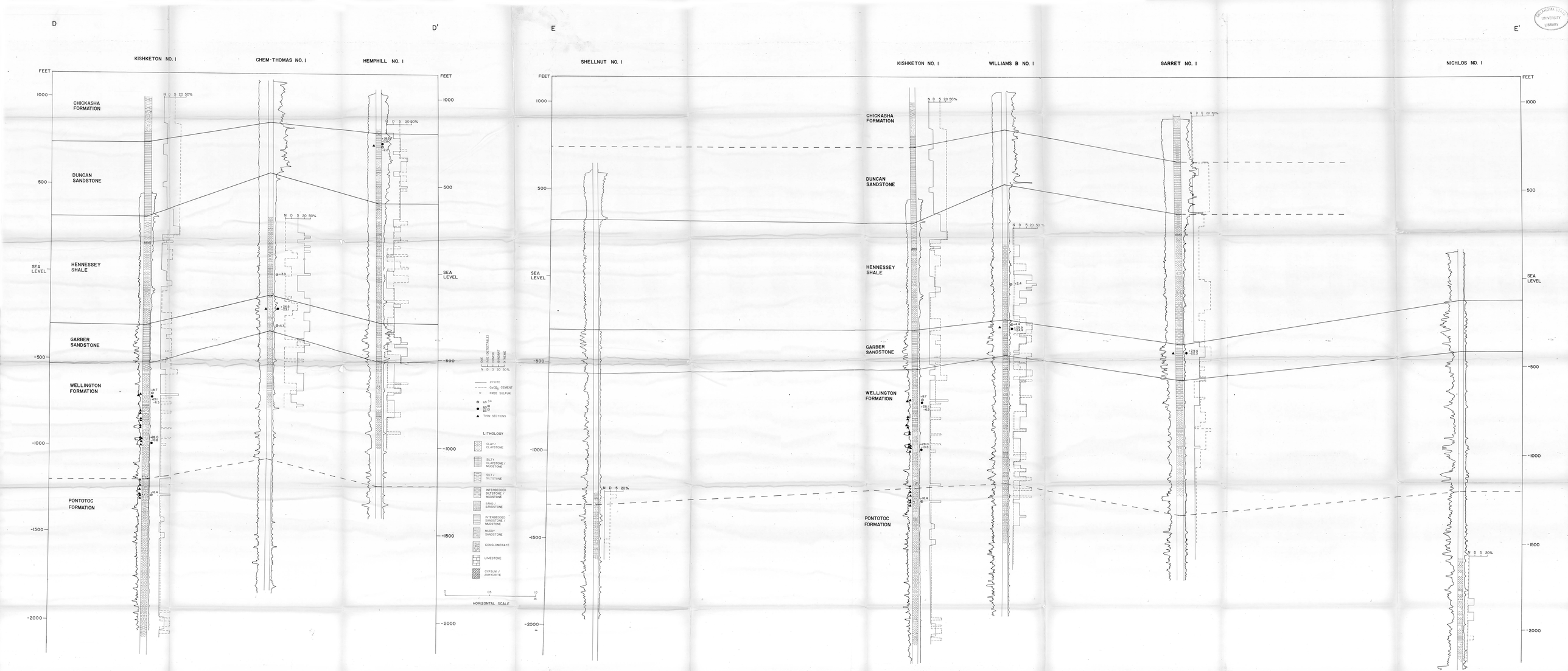

PLATE 3. NORTH-SOUTH CROSS-SECTIONS (D-D' AND E-E') OF THE PERMIAN SECTION AT THE CEMENT-CHICKASHA ANTICLINES

C

C'

GRAY NO. 2

PAU-KUNE NO. 12

KLA-DA-LUG NO. 3

FEET

1000

500

SEA LEVEL

-500

-1000

-1500

-2000

CHICKASHA FORMATION

DUNCAN SANDSTONE

HENNESSEY SHALE

GARBER SANDSTONE

WELLINGTON FORMATION

PONTOTOC FORMATION

N D 5 20 50%

NONE — RARE (DETECTABLE) — COMMON — ABUNDANT — EXTREME

PYRITE

$CaCO_3$ CEMENT

FREE SULFUR

$\%S^{34}$

$\%O^{18}$

$\%C^{13}$

THIN SECTIONS

LITHOLOGY

CLAY / CLAYSTONE

SILTY CLAYSTONE / MUDSTONE

SILT / SILTSTONE

INTERBEDDED SILTSTONE / MUDSTONE

SAND / SANDSTONE

INTERBEDDED SANDSTONE / MUDSTONE

MUDDY SANDSTONE

CONGLOMERATE

LIMESTONE

GYPSUM / ANHYDRITE

0 0.5 1.0 MI

HORIZONTAL SCALE

B

B'

YOUNGBLOOD NO. 1

MELTON NO. 2

HENLEY NO. 2

HARTSHORNE

W. J. WOOD NO. 1

PLATE 2. NORTH-SOUTH CROSS-SECTIONS (B-B' AND C-C') OF THE PERMIAN SECTION AT THE CEMENT-CHICKASHA ANTICLINES